Dissolved organic matter signatures in urban surface waters: spatio-temporal patterns and drivers

Clara Romero González-Quijano[1*], Sonia Herrero Ortega[2], Peter Casper[2], Mark O. Gessner[2,3], Gabriel A. Singer[1,4,5]

[1] Department of Ecohydrology and Biogeochemistry, Leibniz Institute of Freshwater Ecology and Inland Fisheries (IGB), Berlin, Germany

[2] Department of Experimental Limnology, Leibniz Institute of Freshwater Ecology and Inland Fisheries (IGB), Stechlin, Germany

[3] Department of Ecology, Berlin Institute of Technology (TU Berlin), Berlin, Germany

[4] Research Area of Earth, Hanse Wissenschaftskolleg, Delmenhorst, Germany

[5] Department of Ecology, University of Innsbruck, Innsbruck, Austria

**Correspondence to:* clara.romero@igb-berlin.de

Abstract

Advances in analytical chemistry have facilitated the characterization of dissolved organic matter (DOM), which has improved understanding of DOM sources and transformations in surface waters. For urban waters, however, where DOM diversity is likely to be high, the interpretation of DOM signatures is hampered by a lack of ~~basic~~ information on the influence of land cover and anthropogenic factors such as nutrient enrichment and release of organic contaminants. Here we explored the spatiotemporal variation of DOM composition in contrasting urban water bodies, based on ~~spectrophometry~~spectrophotometry and fluorometry, size-exclusion chromatography and ultrahigh-resolution mass spectrometry, to identify linkages between DOM signatures and potential drivers. The highly diverse DOM we observed distinguished lakes and ponds, which are characterized by a high proportion of autochthonous DOM, from rivers and streams ~~with more allochthonous~~where allochthonous DOM is more prevalent. Seasonal variation in DOM composition was apparent in all types of water bodies, ~~driven by~~ apparently due to ~~the~~ interactions between phenology and urban influences~~. Specifically~~, such as~~,~~ nutrient supply, the percentage of green space ~~adjacent~~ surrounding to the water bodies and point source pollution ~~emerged as major urban drivers of DOM composition~~. Optical DOM properties also revealed the influence of effluents from ~~waste water~~wastewater treatment plants, suggesting ~~their~~ that simple optical measurements can be useful in water-quality assessment and monitoring~~.~~ ~~Furthermore, optical measurements~~, informing about processes both within water bodies and ~~in~~ their ~~surroundings,~~catchments~~. which could improve the assessment of ecosystem functioning and integrity.~~

1 Introduction

Urban freshwaters typically receive high loads of organic carbon, nutrients and micropollutants, ranging from pharmaceuticals and personal care products to industrial chemicals and more (Schwarzenbach et al., 2006). Although routine wastewater treatment is increasingly effective, chemical stressors in urban freshwaters remain widespread. Prominent reasons are pollution legacies (Ladwig et al., 2017; Baume and Marcinek, 1993) and continued uncontrolled inputs, particularly by stormwater runoff (Council, 2009). In addition, urban surface waters tend to suffer from severe hydromorphological modifications. This includes the lateral and vertical disconnection from floodplains and aquifers and results in large impacts on the extent and complexity of riverine habitat (White and Walsh, 2020). Furthermore, the disruption of connectivity limits the self-purification capacity of urban surface waters (D'arcy et al., 2007), which can lead to turbid water and visually unpleasant and potentially harmful algal blooms(Carpenter et al., 1998). This and the ~~resulting failure of citizens to recognize~~limited recognition of urban freshwaters as providers of ecosystem services (Huser et al., 2016) calls for improved water management strategies that consider ecological in addition to hygienic and chemical criteria (Gessner et al., 2014).

The concentration and chemical composition of dissolved organic matter (DOM), ~~typically~~generally quantified as dissolved organic carbon (DOC), are key characteristics of aquatic ecosystems. Both concentration and composition are governed by allochthonous inputs and internal biological production and transformation processes (Williams et al., 2016). Typically, however, water quality monitoring only considers concentration and bulk quality properties (e.g. biological oxygen demand, BOD) as measures of DOM availability to, and degradation by, heterotrophic microbes (Jouanneau et al., 2014). This ~~narrow~~ focus is at odds with the extreme diversity of DOM observed in freshwaters, where thousands of compounds can be chemically distinguished (Kellerman et al., 2014; Peter et al., 2020; Stanley et al., 2012). This high diversity and ~~its~~ the strong spatio-temporal variation of DOM composition ~~suggest~~suggests much potential for DOM characteristics to provide insights into the state of freshwater ecosystems in water quality assessment and monitoring. In fact, additional insights into freshwater ecosystems may be gained if the very high diversity of DOM can be used to inform about water quality for ecosystem assessment and monitoring purposes.

Recent progress in analytical methods has increasingly enabled the detailed characterization of DOM to elucidate the sources and fates in surface waters (Xenopoulos et al., 2021). Optical properties can inform not only about the chemical characteristics of DOM but also, for example, about large-scale gradients in aquatic networks (Creed et al., 2015) or the degree of aquatic-terrestrial ecosystem coupling (Sankar et al., 2020; Lambert et al., 2015; Yamashita et al., 2010; Catalán et al., 2013). Fluorescence excitation-emission matrices (EEM) can be processed by parallel factor analysis (PARAFAC) to identify independently fluorescing DOM components (Cory and Mcknight, 2005). Size-exclusion chromatography partitions bulk DOM into molecular size fractions, which also tend to differ in origin and bioavailability (Huber et al., 2011). Finally, the advent of ultrahigh-resolution mass spectrometry (FT-ICR-MS or Orbitrap-MS) has greatly refined the characterization of DOM, revealing associations between compositional turnover of DOM differing in molecular diversity and landscape-scale environmental gradients in lakes (Kellerman et al., 2014) and rivers (Peter et al., 2020).

In the present study we explored variation in the chemical composition of DOM over time and space in contrasting urban surface waters, hypothesizing that a detailed chemical characterization of DOM yields signatures of various human influences. To this end, we explored linkages between chemical ~~DOM~~ composition of DOM and potential drivers determining DOM signatures, including land cover, eutrophication and chemical pollution, which we captured by using a suite of proxies. Our specific goals were to: (i) describe spatio-temporal patterns of DOM composition across a range of urban freshwaters encompassing streams, rivers, ponds and lakes; (ii) identify environmental factors accounting for the observed patterns; and thereby (iii) explore how information on DOM composition could be included in urban freshwater assessment and monitoring~~.~~, complementing approaches and metrics currently used.

2 Methods

2.1 Study sites

The study was conducted in 32 freshwater sites located in the city of Berlin, Germany. Nearly 6.5% of the municipal area (889 km^2) is covered by freshwaters. These comprise 60 lakes (>1 ha), about 500 ponds, the two slow-flowing lowland rivers~~, the Rivers~~ Spree and Havel, and numerous streams, ditches and canals. Selection of the 32 study sites followed a stratified random sampling design (Fig. 1a, ~~Supporting Information~~ Table ~~S1~~A1). Based on geographical information for Berlin`s water bodies, we randomly selected 7 sites in each of 4 strata: lakes, ponds, rivers and streams. Rivers and streams were classified according to a width cutoff of 5 m. Monitoring data on water chemistry (Berlin city administration, SenUVK 2009-2014) were used in a cluster analysis to identify highly polluted sites. These were excluded from the pool used for randomly selecting study sites. ~~Instead, two such rivers (H1 and H2) and two streams (H3 and H4) were deliberately added as polluted sites to lengthen the environmental gradient.~~

Instead, two organically polluted rivers (H1 and H2) and streams (H3 and H4) were deliberately added to lengthen the environmental gradient. Sites H1 and H2 received WWTP effluents (Fig. 1a, Table A2) and sites H3 and H4 presented high levels of diffuse~~d~~ pollution. Other sites for, for some of which monitoring data were unavailable (streams and ponds), were also affected by pollution (Table A1): Pond P4 was formerly connected to an old waste water treatment plant and still receives stormwater inflow during heavy rain events; ~~.~~S5 is located immediately downstream of a WWTP; and R7 became a receiving stream in 2015 (Nega et al., 2019), which was too recent for the site to become classified as polluted based on the monitoring data.~~-~~Land use data obtained from the Berlin city administration (Senate Administration for Environment, 2017) were used to calculate the proportion of paved areas and green spaces within a 50-m perimeter around the selected water bodies using open-source geoinformation software (Qgis Development Team, 2017). The 50-m perimeter was chosen to capture influences in the immediate vicinity of the sites, such as of the riparian zone and slightly beyond, but not of the whole catchments, which are highly variable in size and tend to be difficult to define in urban areas. Delineation of the 50-m perimeter enabled us to distinguish particularly between urban sites adjacent to paved surfaces vs. green spaces. Tufekcioglu (2020) and Johnson (2005) used buffer zones of similar size and a study on ponds using perimeters of up to 3200 m found 50 and 100 m to be most appropriate to assess land-cover effects (Declerck, 2006). ~~We repeatedly sampled all 32 sites in each of four campaigns conducted over an annual cycle, first in spring (April-May 2016), then in summer (July-August 2016), autumn (September-~~

~~October 2016) and winter (February March 2017). We also obtained data on land use from the Berlin city administration(Senate Administration for Environment, 2017), which we used to calculate the proportion of paved and green areas within 50 m buffer strips adjacent to each of the selected water bodies using open source geoinformation software (QGIS Development Team, 2017, Open Source Geospatial Foundation Project. http://qgis.osgeo.org).~~ All samples were taken during base flow conditions (Fig. E1).

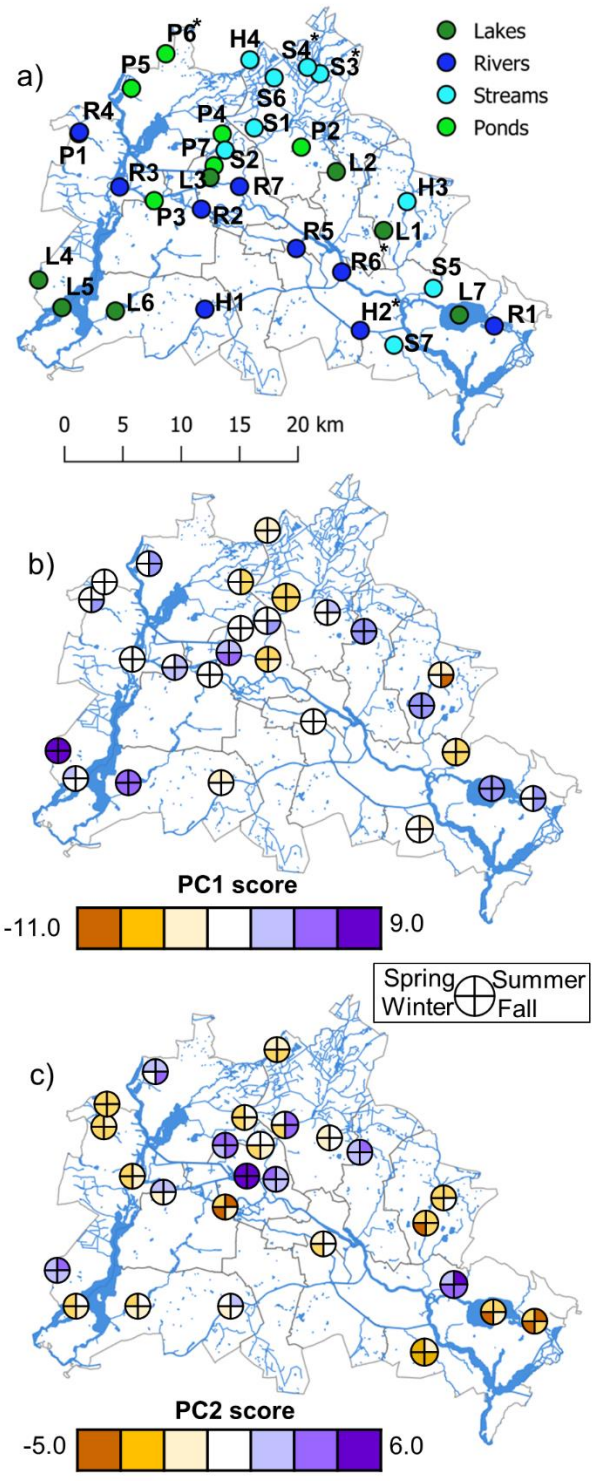
a)
Lakes
Rivers
Streams
Ponds
P6*
H4
S4*
S3*
P5
S6
R4
P4
S1
P2
P1
P7
S2
L2
R3
L3
R7
H3
P3
R2
R5
L1
L4
R6*
S5
L5
L6
H1
L7
H2*
R1
S7
0 5 10 15 20 km
b)
PC1 score
-11.0
9.0
Spring
Summer
Winter
Fall
c)
PC2 score
-5.0
6.0

110

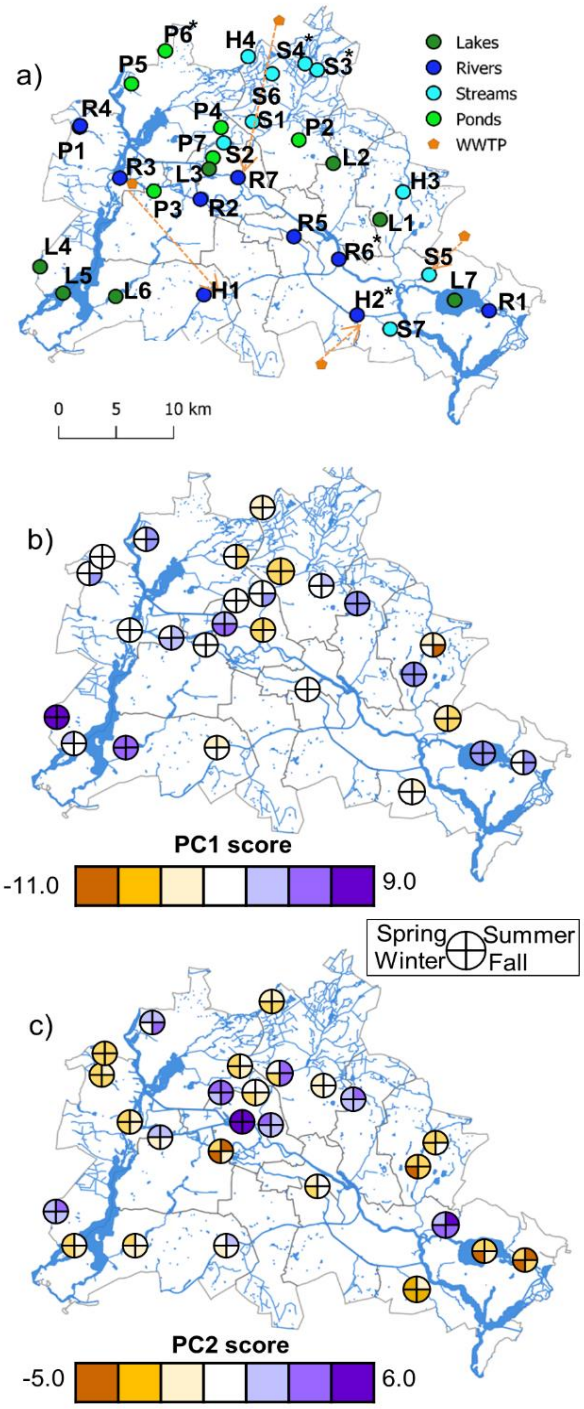

Figure 1 Map of 32 sampling sites in the city of Berlin, including 7 lakes (dark green), 7 ponds (light green), 9 streams (light blue), and 9 rivers (dark blue), including two heavily polluted stream sites and two heavily polluted river sites ~~(a), and PCA scores for these sites in four different seasons (b, c). Site codes are given in Table S1.~~. Wastewater Treatment Plants (WWTP) are shown in orange, arrows point to locations where the effluents are discharged (a). Scores of a Principal Component Analysis (PCA) of DOM characteristics are shown as color gradients for all sites sampled in four seasons (b,c). The PCA is based on DOC concentrations, all absorbance and fluorescence data, absolute component-specific fluorescence intensities from PARAFAC, and data from size-exclusion chromatography. Different colours indicate differences in DOM composition. Site codes are given in Table A1. Sites marked by asterisks (*) were restricted to 3 seasons and hence excluded from the PCA.

2.2 Physico-chemical field measurements and water sampling

We repeatedly sampled all 32 sites in each of four campaigns conducted over an annual cycle, first in spring (April-May 2016), then in summer (July-August 2016), autumn (September-October 2016) and winter (February-March 2017). All field visits occurred during base flow conditions (Fig. E1), ~~During each field visit, w~~We measured water temperature, pH, the dissolved oxygen (DO) concentration and electrical conductivity using a hand-held WTW Multiprobe 3320 (pH320, OxiCal-SL, Cond340i, Weilheim, Germany) or a smarTROLL probe (In-Situ, Fort Collins, CO, USA). We also collected integrative water samples (2 L) from the upper 0.5 m water layer for chlorophyll-*a* and DOM analyses. The water was kept cool in acid-washed polycarbonate Nalgene bottles placed in a cooling box pending filtration in the laboratory (GF75, 0.3 µm average pore size; Advantec, Tokyo, Japan) within 6 hours after sampling. Additional volumes of surface water were filtered through pre-combusted glass fiber filters (GF75) directly in the field. These filters were placed ~~into~~in acid-washed, pre-combusted (450 °C, ~~4h~~4 h) glass vials (15-20 mL) sealed with a PTFE septum in a screw-cap for later measurements of dissolved organic carbon (DOC) concentrations, DOM fluorescence and absorbance, and DOM molecular size distribution. The water passed through the filter was collected in acid-washed polyethylene tubes for analyses of soluble reactive phosphorus (SRP), nitrate (NO_3^-), nitrite (NO_2^-), ammonium (NH_4^+) and trace organic compounds (TrOCs). We also took unfiltered water samples for total phosphorus (TP) analysis. For each variable, we collected three replicate samples at each site in each season. We stored all samples in the dark in a cooling box during transport. To preserve samples and remove all inorganic carbon, we acidified (pH 2) the water for DOC, NO_3^-, NO_2^- and NH_4^+ analyses with 2 M HCl within 6 hours after sample collection. DOC concentrations and DOM fluorescence and absorbance were measured within 24 h. Filtered water for analyses of SRP, NO_3^-, NO_2^-, NH_4^+ and TrOCs was frozen at -20 °C.

2.3 DOM characterization

We determined total DOC concentrations by high-temperature catalytic combustion and infrared spectrometry on a TOC-V Analyzer (Shimadzu, Kyoto, Japan), with a 0.5 mg L^{-1} limit of quantification and a typical analytical precision of 3%. DOM absorbance and fluorescence were simultaneously determined on an Aqualog instrument (Horiba Ltd, Kyoto, Japan~~). We used the absorbance spectra to calculate several indexes (Table A2~~) using ultra-pure water as a blank. ~~-~~From each site and season, we measured three analytical replicates of each of the three independent samples. ~~w~~We generated nine measurements (each of three process replicates was measured 3 times) immediately after 3 blanks. The high level of replication allowed identification of artefactual measurements and outlier removal following a visual check of absorbance spectra and fluorescence excitation-emission matrices (EEMs). The ~~F~~fluorescence data was expressed in Raman units, removing the need for an external quantification standard. ~~w~~

Iron can form stable complexes with DOC and interfere with optical DOC measurements, so that the two variables are not independent (Maranger et al., 2003). We found that the quotient of light absorbance at 420 nm (a_{420}) and DOC concentration, a measure of the optical signal returned per unit DOC (Weyhenmeyer et al., 2014), was indeed significantly correlated ($p = 0.002$) with the Fe concentration measured in the monitoring program of the Senate of Berlin in two of our lakes (L5 and L7: 0.06 ± 0.03 mg/L), four of the rivers (H1, R1, R6 and R7: 0.30 ± 0.14) and two of the streams (H3 and H4: 0.31 ± 0.14). The relationship explained 31% of the overall variation (Fig. E2).

Consequently, Fe could have influenced our optical estimates of DOC concentration. However, because our analysis rests on differences in DOM composition as opposed to concentration (see below), it is unlikely that the presence of Fe notably influenced the spatial and temporal patterns observed in our study.

We calculated several indices from the absorbance spectra (Table B2): the specific UV absorption ($SUVA_{254}$) as a proxy for DOM aromaticity (Weishaar et al., 2003), the ratio of absorbance at 250 and 365 nm (E2:E3) as an (inverse) indicator of molecular size (Peuravuori and Pihlaja, 1997), the ratio of E4:E6 as an indicator of humification (Chen et al., 1977)~~, the short-wavelength slope within the wavelength region of 275-295 nm (Helms et al., 2008) as an inverse correlate with molecular weight and aromaticity,~~, and the ratio of slopes (SR) computed from short and long wavelength regions (Loiselle et al., 2009) as another negative correlate with DOM molecular weight. We used the fluorescence data to compute the freshness index β/α (Table ~~A2~~B2) (Wilson and Xenopoulos, 2009), which indicates the relative importance of recently produced DOM (Parlanti et al., 2000). Furthermore, we calculated the fluorescence index (~~FIX~~FI) as the ratio of fluorescence intensities at the emission wavelengths of 470 and 520 nm (obtained at an excitation wavelength of 370 nm), which has proved useful to distinguish the relative contributions of terrestrial ~~(FIX~1.4) and aquatic (FIX~1.9) sources of DOM (Mcknight et al., 2001).~~plants (FI~1.2) and microbes or algae (FI~1.4) as sources of DOM (Cory et al., 2010; Cory and Mcknight, 2005; Jaffé et al., 2008; Fellman et al., 2010). Finally, we computed the humification index (HIX) as a proxy for humic substances (Ohno, 2002). ~~Fluorescence excitation-emission matrices (EEMs)~~ EEMs were used for PARAFAC ~~analysis~~, a multivariate three-way modeling approach decomposing EEMs into individual fluorophores (Bro, 1997; Stedmon and Bro, 2008). We derived ~~8~~7 components from a total of 116 EEMs and compared their loading spectra with the OpenChrom/OpenFluor database (http://www.openfluor.org) (Murphy et al., 2014). ~~See Supporting Information for details of data processing, including PARAFAC analysis.~~

Prior to PARAFAC, we interpolated missing data in Rayleigh scatter regions to expedite the modeling process (Bro, 1997). The calculations for PARAFAC were performed using Matlab (version 7.11.0, MathWorks) and the DOMFluor Toolbox (1.7) following Stedmon & Bro (2008). We limited the number of components to 10, rigorously checked residual EEM plots, and assessed the final models by split-half validation (Fig. B1) as recommended by Stedmon and Bro (2008).

The molecular size distribution of DOM was analyzed by liquid size-exclusion chromatography in combination with UV and IR detection of organic carbon and UV detection of organic nitrogen (LC-OCD-OND) (Huber et al., 2011). The instrument was calibrated with IHSS Suwannee River I Humic Acid and Fulvic Acid standards (International Humic Substance Society, St Paul, MN, USA). Carbon and nitrogen detectors were calibrated with potassium hydrogen phthalate (C) and sodium nitrate (N). Limits of quantification were 0.1 mg C L^{-1}, and 0.01 mg N L^{-1}, analytical precision ~~of~~based on repeated standard measurements was better than 3%. We determined concentrations of three molecular size fractions: humic-like substances (HS-C and HS-N reported in mg C L^{-1} and mg N L^{-1}, respectively), high-molecular weight non-humic substances (reported as HMWS-C and HMWS-N, in mg C L^{-1} and mg N L^{-1}) and low-molecular weight substances (LMWS, in mg C L^{-1}).

To examine the molecular composition of DOM, we used ultrahigh-resolution Fourier-Transform Ion Cyclotron Mass Spectrometry (FT-ICR-MS). ~~We extracted DOM on Agilent Bond Elut PPL solid-phase columns (Dittmar et al., 2008) from 1 L of filtered water acidified to pH 2.~~We extracted DOM on Agilent Bond Elut PPL solid-phase columns (Dittmar et al., 2008) from 1 L of filtered water acidified to pH 2. We then diluted extracts to 10 µg L^{-1} C in 1/1 ultrapure water/methanol before broadband mass spectrometry on a 15 Tesla Solarix FT-ICR-MS (Bruker Daltonics, Bremen, Germany) in electrospray ionization negative mode (300 accumulated scans, ion accumulation time of 0.1 s, flow rate of 240 µL/h). We performed internal mass calibration and exported the raw mass lists from 150 to 1000 Da for further data processing using previously established R code (Del Campo et al., 2019). ~~Briefly, we first applied a method detection limit similar to Riedel & Dittmar (Riedel and Dittmar, 2014) before aligning m/z values across samples (Del Campo et al., 2019).~~Briefly, we first applied a method detection limit similar to Riedel & Dittmar (2014) before aligning m/z values across samples (Del Campo et al., 2019). Subsequently, we assigned chemical formulas to mean m/z values assuming single-charged deprotonated molecular ions and Cl-adducts for a maximum elemental combination of $C_{100}H_{250}O_{80}N_4P_2S_2$, respecting chemical constraints~~ and using rigorous mass error assessments, stable isotope confirmation and homologous series assessment (Del Campo et al., 2019). More detail of the FT-ICR-MS methods can be found in the Supplement material. To condense the mass spectrometric information, we derived 12 molecular groups~~. To eliminate doubtful formula assignments, we performed (i) an accurate assessment of mass error including its partitioning into random and systematic components (Savory et al., 2011): (ii) an exploration for stable isotope validation by daughter peaks (Koch et al., 2007), and (iii) a homologous series assessment based on CH_2, CO_2 and H_2O as chemical building blocks for aliphatic, acid-based and alcohol-based elongation (Koch et al., 2007). To condense the mass-spectrometric data, we grouped formulas into 12 non-overlapping molecular groups (Lesaulnier et al., 2017) based on elemental composition and calculated the average molecular mass, number of formulas (molecular richness) and total intensity for each of them. In addition, we computed the double-bond equivalents (DBE) and the aromaticity index (AI) as indicators of unsaturated compounds~~ (Koch and Dittmar, 2006)~~, and the molecular lability boundary (MLB) as a measure of lability~~ (D'andrilli et al., 2015)~~. Finally, we used van Krevelen plots to present the sum formulas derived from the FT-ICR-MS data in a space defined by O:C (oxygen richness) and H:C (saturation) ratios. We used random order of plotting to avoid bias due to systematic overplotting of thousands of compounds with identical O:C and H:C ratios.

2.4 Additional water-chemical analyses

~~We determined total DOC concentrations by high-temperature catalytic combustion and infrared spectrometry on a TOC-V Analyzer (Shimadzu, Kyoto, Japan).~~ NO_3^-, NO_2^- and NH_4^+ were analyzed on a FIAcompact (MLE GmbH, Dresden, Germany). TP was measured using the same technique with unfiltered water samples that were digested with $K_2S_2O_8$ (30 min at 134 °C). We measured chlorophyll-*a* concentrations spectrophotometrically (HITACHI U2900~~;~~ ~~Tokyo, Japan) following hot ethanol extraction (Jespersen and Christoffersen, 1987)~~, Tokyo, Japan) following hot ethanol extraction (Jespersen and Christoffersen, 1987) of three GF75 filters from each individual water sample. Concentrations of 18 trace organic compounds (TrOCs) were determined by HPLC-MS/MS (Shimadzu, Kyoto, Japan)

(Zietzschmann et al., 2016). These included chemicals such as acesulfame (a sweetener), benzotriazole (a corrosion inhibitor), and drug residues like carbamazepine and gabapentin (Table ~~B1~~C1).

2.5 Data analysis

We used repeated-measures ANOVA to test for differences among types of water bodies and ~~seasonal~~ sampling periods (referred to as seasons hereafter) for a variety of response variables; ~~there was non significant~~ as the interaction between water body type and season~~. Further~~ was not significant we recomputed models including main effects only. Furthermore, we assessed the importance of seasonal variation in each water body type by computing a respective variance component using a type-II ANOVA (aka variance component analysis) for data from each water body type with season and site ~~-~~ID as random factors; this approach ~~assesses~~facilitates the assessment of temporal variation as a fraction of total variation within each water body type. Normal distribution was assessed graphically by quantile plots and histograms. For ANOVA, data were log(x) or √x -transformed to achieve conditions of normality and variance homogeneity of the residuals.

For constrained multivariate analyses we considered land cover adjacent to the water bodies, trophic state and micropollutant load as drivers of variation in DOM chemical composition. We used the percentages of urban green space and paved areas as ~~a proxy~~proxies for land cover~~ and assessed trophic state based on,~~ concentrations of TP, NH_4^+, NO_3^- and chlorophyll *a*~~. Finally,~~ as a measure of trophic state; and the ~~first axis of a principal component analysis (PCA) based on the~~ mean TrOC ~~dataset was used~~concentration ~~-~~as a proxy for micropollutant load. We also performed a principal component analysis with all the TrOCs.~~.~~

We followed a three-step approach to analyze the spatio-temporal patterns of DOM composition: First we identified major axes of variation in DOM composition by a PCA based on quantitative indicators of DOM, analytically accessible fractions thereof or quantitative proxies: DOC concentration, all absorbance and fluorescence ~~data, absolute~~indices, component-specific fluorescence intensities from PARAFAC normalized to DOC, and the ~~results from~~ size-exclusion chromatography data. Only the 27 sites sampled in all four seasons were included in this analysis. All variables were standardized to a mean of zero with a variance of 1 to ensure equal ~~weightings~~weighting, and projected onto the ordination space using Pearson correlations of the variables with PCA axes in a distance biplot (*sensu* Legendre and Legendre ~~(~~, 2012). To explore spatial patterns, we mapped PC1 and PC2 scores onto Berlin´s landscape using QGIS (QGIS Development Team, 2017~~, Open Source Geospatial Foundation Project; http://qgis.osgeo.org). ~~).

Second, we used the same dataset as the dependent matrix in a redundancy analysis (RDA) with the set of potential drivers described above used as predictor variables. The goal of the RDA was to identify potential drivers of DOM composition and thereby assess, reciprocally, whether various DOM descriptors are ecologically informative. We started with the full RDA model and forward-selected drivers (Legendre and Legendre, 2012). For hypothesis tests in the RDA, permutations were restricted to account for repeated measurements at the same sites across seasons by first permuting sets of four seasonal measurements across sites and then permuting across seasons within each site. To check our ability to identify drivers behind major variation observed in DOM composition, we used Procrustes analysis

to assess the similarity of PCA and RDA ordinations, including a permutation-based test of the non-randomness of the achieved superimposition (Mardia, 1979; Peres-Neto and Jackson, 2001).

Third, we exploited results of the FT-ICR-MS to facilitate interpretation of the two major axes of variation in DOM chemical composition resulting from the PCA. The FT-ICR-MS data were only available for three seasons and were purely compositional (relative intensities), as the many thousands of compounds contained in the spectra cannot be calibrated to yield concentrations. To link the quantitative and compositional datasets, we correlated PCA scores ~~of PCA axes~~ with compound-specific relative intensities of the mass spectra. The compound-specific correlation coefficients were then used as ~~color~~colour codes in van Krevelen plots~~, which locate chemical formulae identified by FT-ICR-MS in a space defined by oxygen richness (O:C) and saturation (H:C).~~. FT-ICR-MS-derived information such as the richness or average weight of specific molecular groups ~~were~~was also projected onto the PCA ordination space as arrows, provided correlation coefficients were >0.2. All statistical analyses and graphs were made with R 3.2.4 ~~(R Core Team, 2016).~~(R Core Team, 2016).

3. Results

3.1 Physico-chemical characteristics

Among all physico-chemical variables, only DOC concentration and temperature differed significantly among types of water bodies ($p<0.05$ and $p<0.001$, respectively). Temperature varied strongly across seasons, but still proved significantly different among water body types, with lakes and rivers being warmer than ponds and streams. DOC concentrations did not vary across seasons, but were significantly higher in ponds and streams than in lakes and rivers. Ponds also showed the highest chlorophyll-*a* concentrations and rivers the lowest, but these differences were not significant.

Separate ANOVAs for each water body type showed that seasonal variation in TP and NH_4^+ concentrations was highest in rivers and streams~~.~~ (Table B1). Seasonal variation in NO_3^- concentrations was generally high, but systematic differences were neither detected among seasons nor sites (Table ~~A1~~B1). Seasonal variation of chlorophyll-*a* concentrations was also high and similar across types of water bodies.

The analysis of TrOCs identified acesulfame, a widely used artificial sweetener ~~(Buerge et al., 2009), in 72 out of a total of 120 samples taken at 32 sites across all seasons (Table B1). Similarly, two corrosion inhibitors included in the analysis~~(Buerge et al., 2009), in 72 out of a total of 120 samples taken at 32 sites across all seasons (Table C1). Similarly, two corrosion inhibitors, benzotriazole and methylbenzotriazole (Cotton and Scholes, 1967; Tamil Selvi et al., 2003), occurred in 68 and 63 samples, respectively. Fifteen other TrOCs were detected in at least 2 and up to 62 samples (Table ~~B1~~C1). Rivers showed the highest concentrations throughout the year. The first principal component of the PCA considering all TrOCs explained 61% of the total variance (Fig. ~~B1~~C1) and separated streams and rivers with higher concentrations from ponds and lakes where concentrations of TrOCs were lower and often undetectable, particularly in ponds (Table ~~B2).~~C2). The strong positive correlations between most of the TrOCs suggested the applicability of a simple average TrOC concentration as a proxy for micropollutant load in further analysis; this mean was computed across all TrOCs after z-standardization of each TrOC for equal weighting.

3.2 DOM composition

PARAFAC modeling resulted in ~~8~~7 components referred to as C1-~~C8~~C7 (Table ~~A3~~B3, Fig. ~~A1~~B1). Components C6 and ~~C8~~C7 were previously found to be protein-like, whereas all other components have been reported as humic-like (Table ~~A3~~B3). In contrast to the standard physico-chemical variables ~~we measured~~ and ~~the~~ results from size-exclusion chromatography (Table ~~A6~~B6), the PARAFAC components and absorbance and fluorescence indices generally showed significant differences among water body types (Table ~~A4~~B4 and ~~A5~~B5).

The first axis of the PCA analyzing spatio-temporal patterns of DOM chemical composition explained ~~36~~34% of the total variance (Fig. 2). PC1 was largely defined by the negative loadings for ~~C2~~C1 and ~~C1~~C2 (representing humic substances originating from ~~waste water~~wastewater treatment), ~~the short wavelength slope,~~ $SUVA_{254}$ and LMWS (Fig. 2b). Furthermore, PC1 correlated positively with the absorption slope ratio, E2:E3 (molecular size), β/α and HMWS-C. This axis separated water body types, from lakes on the right to ponds, rivers, and finally streams on the left. The optical proxies identified PC1 as a gradient spanning from lakes, where DOM had lower aromaticity and contained more freshly produced material, to streams, which showed high aromaticity and low proportions of fresh DOM. Pond P4, which was identified as an outlier because of particularly high NH_4^+ concentrations, also showed a rather distinct DOM composition.

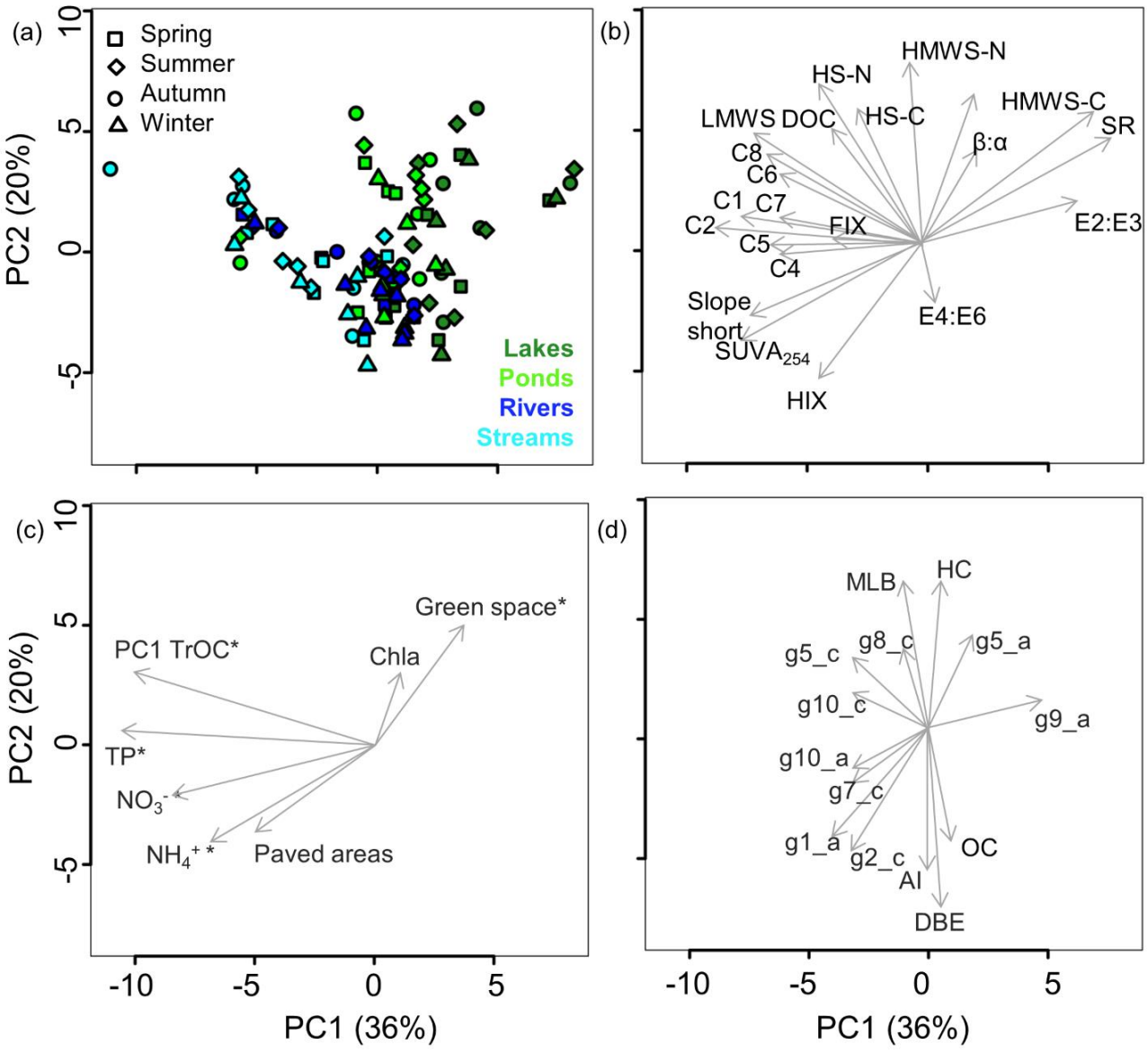
(a)
Spring
Summer
Autumn
Winter
Lakes
Ponds
Rivers
Streams
PC2 (20%)
(b)
HMWS-N
HS-N
HMWS-C
LMWS DOC
HS-C
SR
β:α
C8
C6
C1
C7
C2
FIX
E2:E3
C5
C4
Slope
short
E4:E6
SUVA254
HIX
(c)
Green space*
PC1 TrOC*
Chla
TP*
NO3-*
NH4+*
Paved areas
PC2 (20%)
PC1 (36%)
(d)
MLB
HC
g5_c
g8_c
g5_a
g10_c
g9_a
g10_a
g7_c
g1_a
g2_c
OC
AI
DBE
PC1 (36%)

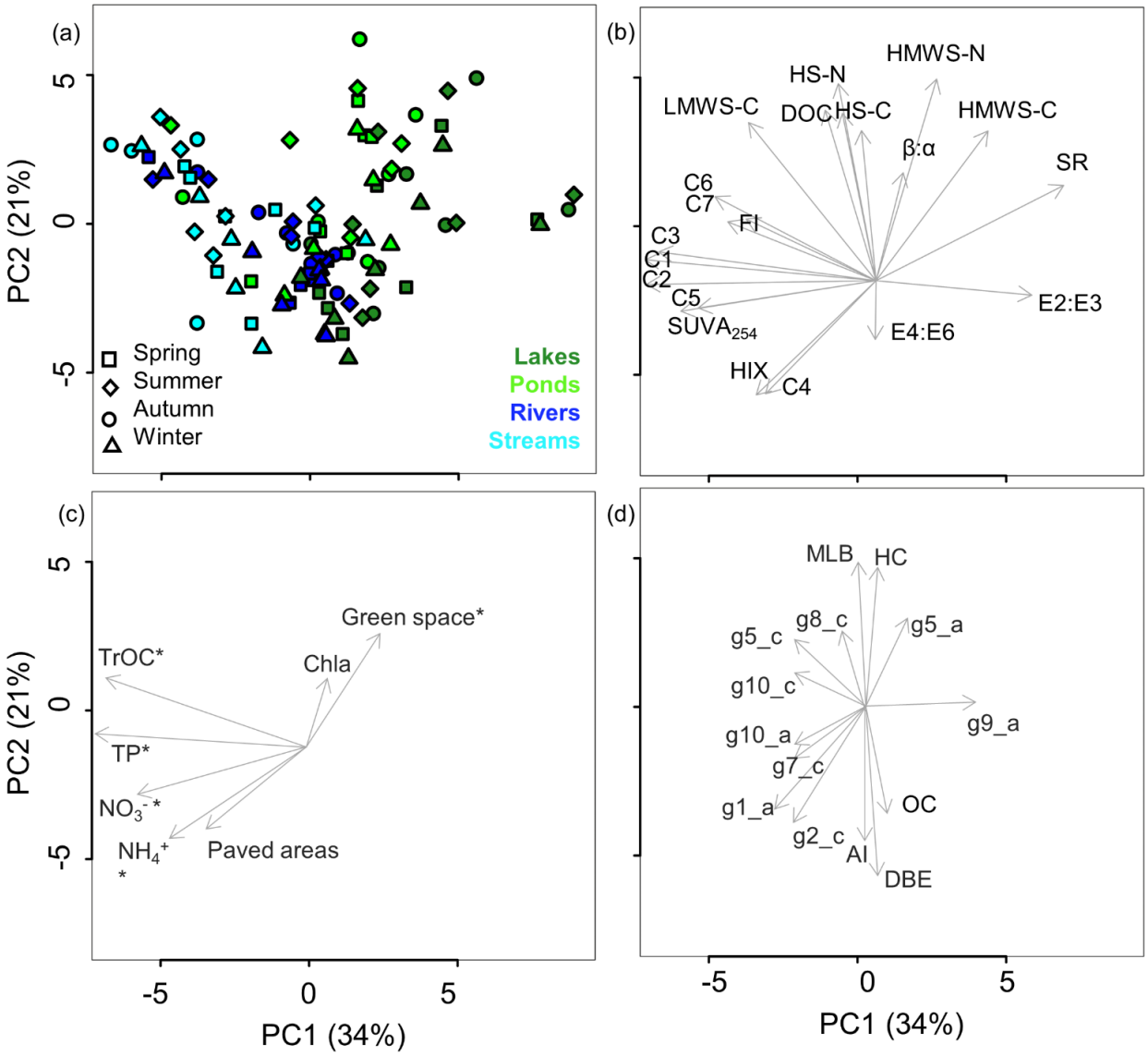

Figure 2 Ordination of sites (a) by PCA based on DOM characteristics (b): (i) indices derived from measurements of absorbance (E2:E3 indicating molecular size, E4:E6 representing the humification ratio, the slope ratio SR, and $SUVA_{254}$) and fluorescence (freshness index β:α, fluorescence index ~~FIX, short wavelength slope~~FI, and humification index HIX), (ii) PARAFAC components C1 to ~~C8~~C7, and (iii) data from size exclusion chromatography (humic-like substances HS, high-molecular weight non-humic substances HMWS, low-molecular weight substances LMWS). (c) ~~RDA~~Potential drivers of DOM composition, that were used as constraints in the RDA, were mapped onto the PCA ordination, with the significant constraints marked by an asterisk (*). (d) FT-ICR-MS-derived indices and molecular groups mapped onto the PCA ordination representing only groups correlated with PC1 or PC2 (r>0.2; oxygen richness O:C, saturation level indicated by H:C, double-bond equivalents DBE, aromaticity index AI, molecular lability boundary MLB, molecular groups g1 and g2 indicating black carbon without and with heteroatoms, g5 consisting of unsaturated aliphatics, g7 representing saturated fatty acids, g8 and g9 denoting carbohydrates without and with heteroatoms N, S or P, and g10 comprising peptides). The molecular group measures are either average masses (marked by '_~~am~~a') or counts of molecules (marked by '_c'~~co~~).

PC2 explained an additional ~~20~~21% of the total variance and correlated positively with HMWS (mg N/L) and β/α, and negatively with HIX. An exploration of spatio-temporal variation by plotting site-specific PC scores (Fig. 3) identified PC2 as the axis capturing temporal variation, with the four seasons aligning vertically at most sites. Winter and summer had the lowest and highest PC2 scores, respectively, with transitional seasons located in between. Thus, higher proportions of humic substances in winter contrast with more labile DOM in summer. In agreement with the variable-specific seasonal variance components, the degree of seasonal differentiation differed among water body types also in multivariate space, being higher in streams and ponds than in the larger lakes and rivers (Fig. 3b). Except for ~~sites P4 and~~site H3~~, two water bodies behaving exceptionally also in many other respects~~, seasonal variability was poorly reflected by PC1, which largely captured variation among individual water bodies or water body types, separating flowing from standing waters. Visual inspection of PCA scores mapped across Berlin (Fig. 1b,c) did not reveal a spatial signature transcending types of water bodies. RDA identified the areal percentage of green space adjacent to the water bodies, TP, NH_4^+, NO_3^- and the ~~first axis of the PCA based on TrOCs~~mean TrOC concentration as significant predictors of DOM composition (Fig. ~~C1~~D1). The resulting PCA and RDA ordinations for DOM were ~~significantly~~strongly correlated (Procrustes rotation 0.73, $p<0.001$), suggesting that the considered predictors were indeed major drivers of variation in DOM chemical composition.

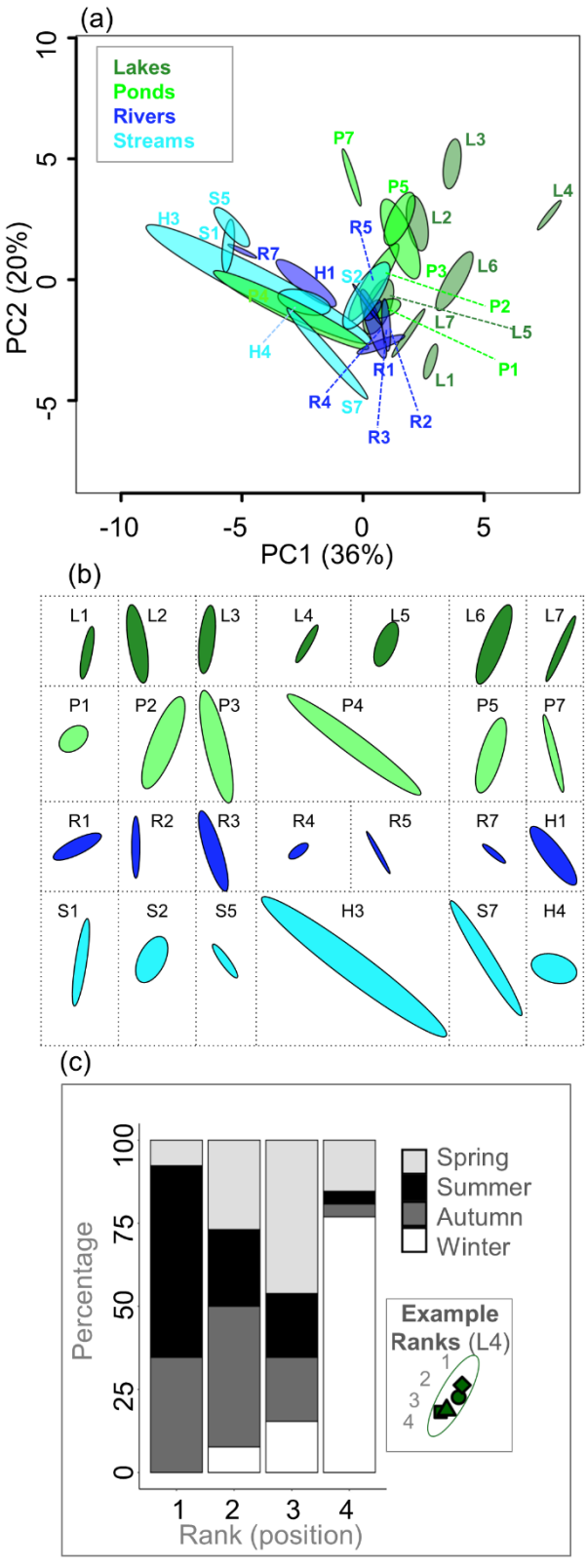
(a)
Lakes
Ponds
Rivers
Streams
PC2 (20%)
PC1 (36%)
(b)
(c)
Spring
Summer
Autumn
Winter
Example
Ranks (L4)
Percentage
Rank (position)

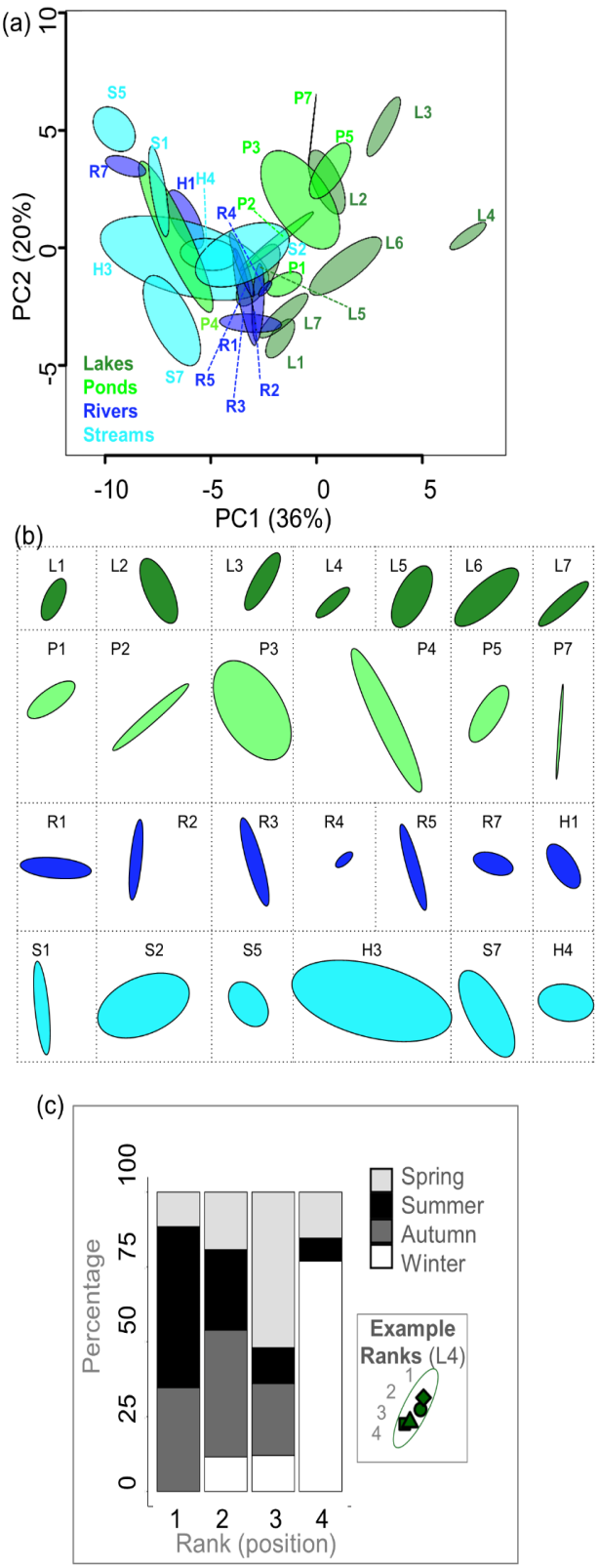
(a)
PC2 (20%)
PC1 (36%)
Lakes
Ponds
Rivers
Streams
(b)
(c)
Percentage
Rank (position)
Spring
Summer
Autumn
Winter
Example Ranks (L4)

345

Figure 3 (a) PCA biplot based on DOM absorbance and fluorescence indices, PARAFAC components and size exclusion chromatography data from 4 contrasting types of urban freshwater bodies, including lakes, ponds, rivers, and streams, in addition to two streams and two rivers specifically selected as highly polluted sites. Each of the ellipses represents one sampling site that was visited 4 times, once in each season. Site codes are given in Table ~~S1~~A1. (b) Visual comparison of site-specific seasonal variation based on the size, shape and orientation of ellipses, plotted separately per site. (c) Seasonal variation across sites illustrated by ranking the sampling dates at each site according to the PC2 scores, as shown in the inset. The stacked histograms show frequencies of the seasons across the four ranks. Summer samples tend to produce high scores at most sampling sites, whereas winter samples tend to score low.

High-resolution mass spectrometric analyses of samples from three seasons provided additional insights into the chemical composition of DOM. Overall, we detected 6446 molecular formulas, most of them representing molecular groups typical of humic material derived from soils. This includes highly unsaturated O-rich compounds, polyphenols and other aromatic structures, followed by unsaturated aliphatic polyphenols, and polycyclic aromatic compounds~~es~~ with aliphatic chains. The van Krevelen plots revealed a positive correlation of lignin-like molecules and carbohydrates with PC1 of DOM and identified these molecules as abundant in lakes (Fig. ~~A2~~B2). In contrast, the negative association of proteins with PC1 was typical of streams. Information on the molecular groups identified by FT-ICR-MS and projected on the PCA space (Fig. 2d) showed carbohydrates and sugars containing N, S or P to be positively related to PC1. Furthermore, PC1 was negatively related to black carbon, polyphenols and polycyclic aromatic compounds with aliphatic chains, which are all typical of soil-derived humic material, as well as with unsaturated aliphatics, saturated fatty acids and peptides, indicating that all of these molecular groups were more important in streams. Lastly, the computed molecular lability boundary (MLB), carbohydrates, sugars without heteroatoms (N, S or P) and unsaturated aliphatics were positively related to PC2, while AI, DBE, black carbon and polyphenols were negatively related to PC2.

4. Discussion

4.1 Spatial patterns and drivers of DOM signatures

Our results show that the chemical composition of DOM in contrasting surface waters of the metropolitan area of Berlin, Germany, is highly diverse. This reflects both aquatic-terrestrial linkages and DOM transformations within the aquatic systems (Fonvielle et al., 2021) ~~and suggests a high ecosystem-level functional diversity across the urban aquatic network.~~ Clear differences among the four types of water bodies we investigated were due to distinct signatures of streams and rivers vs. ponds and lakes. This was revealed especially by the first principal component (PC1) of a PCA (Fig. 2), which reflects the dominant gradient defined by variation in DOM composition across the 32 urban sites included in the study. Since optical measurements play an important role in our analysis of DOM, it is important to consider potential interference by iron. Elevated iron concentrations lead to brownification, similar to effects of allochthonous DOM, and Fe and DOC also form stable complexes, so that the two variables are not independent (Maranger et al, 2003). However, Fe data available from the Senate of Berlin for two of our lakes (L5 and L7: 0.06 ± 0.03 mg/L), four of the rivers (H1, R1, R6 and R7: 0.30 ± 0.14) and two of the streams (H3 and H4: 0.31 ± 0.14), all concentrations were below the threshold of 1 mg/L, suggesting that Fe increases may result in a420/DOC increases (Weyhenmeyer et al, 2014).

Stream DOM exhibited higher aromaticity (as indicated by $SUVA_{254}$) and lower amounts of recently produced, low-molecular DOM (as indicated by the freshness index or the slope ratio) than lakes at the opposite end of the gradient. This pattern matches results from agricultural streams near Berlin, where $SUVA_{254}$ values up to 3 L m^{-1} mg^{-1} ~~have been~~were reported (Graeber et al., 2012) and from an urban river in southwestern Korea ($SUVA_{254}$ values of 2.5 L m^{-1} mg^{-1}) (Park, 2009). The distinct signature is also reflected in other DOM components, such as the fluorophore C2, which was more important in streams and identified as terrestrial humic material (Murphy et al., 2011). Streams also showed higher levels of humic-like (C1) and protein-like (~~C8~~C7) compounds, whereas higher values of the freshness index characterized lakes. These patterns consistently indicate that the arrangement of sites along PC1 reflects a gradient of allochthonous vs autochthonous sources of DOM. A corollary of this finding is that despite the potentially pervasive influence of the urbanized surroundings, urban streams in particular are more tightly linked to the terrestrial environment than urban lakes, just as is the case for flowing and standing waters in natural landscapes (Larson et al., 2014).

In contrast to natural landscapes, however, the linkage of urban waters with their terrestrial surroundings is mediated by paved surfaces and engineered flow paths, including roof run-off into rain gutters, extensive (partially leaky) sanitation networks and sewage overflows in WWTPs that are activated following heavy rainfall or snowmelt. The urban gradient from allochthonous to autochthonous DOM sources we document could thus be driven by surface run-off rather than soil seepage and subsequent delivery of DOM to surface waters via groundwater. Although we did not sample after major storms (Fig. E1), we would expect legacy effects of past runoff events to differ among sites, depending on the extent of green space and impervious surface area in the surroundings of the sites. ~~.~~ This interpretation is supported by higher levels of proteins (Fig. 2) characterizing the urban streams and rivers, as opposed to soil-derived humic DOM signatures typical of unimpacted streams and rivers (Hutchins et al., 2017). The proteins could originate from surface runoff integrating various sources of urban pollution but they might also derive from WWTPs, as implied by the nature of some of the PARAFAC components ~~we identified~~ (Table ~~A3~~B3). For instance, the humic fluorophore C2 has been reported in WWTP effluents that may be discharged into urban surface waters (Murphy et al., 2011). Point-source inputs were also identified as drivers of DOM composition by the influence of TrOCs in our RDA and their correlations with C2 and ~~C8~~C7, all of which are components of WWTP effluents.

Lakes differ from streams by a typically greater importance of autochthonous production. Since this production is fostered by abundant ~~nutrients. Elevated~~nutrient supply (given sufficient light), elevated nutrient concentrations should ~~hence~~ coincide with DOM signatures indicative of autochthonous carbon ~~sources, as~~sources. This pattern has been found in agricultural streams, where the freshness index β:α indicating autotrophic activity was related to high nitrogen concentrations (Wilson and Xenopoulos, 2009). ~~This pattern~~However, it contrasts with the negative relation between nitrogen concentration and the proportion of fresh DOM found across our study sites, where high nutrient concentrations were instead strongly related to DOM components of WWTP effluents. This typically resulted in an allochthonous DOM character at high-nitrogen sites. Notably, signatures like lower β/α in WWTP-impacted sites may also be a consequence of the highly processed nature of DOM that underwent degradation in a WWTP.

Similarly, the TP concentration was significantly related to DOM composition in our RDA, where phosphorus-rich water bodies also proved to have more allochthonous than autochthonous DOM. This points to inputs from urban surface runoff rather than groundwater inflow where long flow paths and residence times provide ample opportunities for phosphorus immobilization. As with N, additional phosphorus may derive from WWTP effluents, as suggested by the positive relationship between TP concentration and the fluorophore C2 as a putative tracer of WWTP effluents (Murphy et al., 2011). Overall, the negative relationships between nutrient availability and the importance of autochthonous components in the DOM pool suggests that while streams and rivers may efficiently collect N and P from the urban environment; lakes are more efficient at channeling nutrients into autochthonous production. Thus, the autochthonous DOM signature in urban lakes appears to be largely independent of nutrient supply and rather be facilitated by longer water residence times, higher water temperature and favorable light conditions.

Our results on urban surfaces driving urban allochthonous DOM composition meet our expectation that land cover notably influences the composition of DOM in urban surface waters (Williams et al., 2016; Sankar et al., 2020). This conclusion is supported by results ~~from~~of our RDA, which identified the presence of green spaces in the perimeter of the water bodies as a significant influence. However, the relationship between land cover and DOM composition must be interpreted with caution because all lakes were situated in areas with green spaces in their surroundings, whereas streams ran through areas dominated by buildings and paved surfaces. The urban running waters, more than lakes and ponds, thus received high surface runoff during rain events, including high inputs of pollutants and allochthonous DOM. ~~Given the evident negative relationship between green space and paved surface areas (R^2 = 0.47, $p<0.001$), green spaces might be used as an inverse proxy for paved surfaces influencing DOM signatures in urban surface waters. However, since paved surface area per se did not emerge as a significant predictor in our RDA, land cover can at best partly account for the observed variation in DOM composition across the contrasting urban sites we investigated.~~

Except for ponds and some lakes, all investigated water bodies had direct surface water connections, which could result in spatial autocorrelation (Peterson et al., 2006b; Peterson et al., 2006a). In addition, spatial patterns may arise from the prominent land cover gradients in Berlin, ranging from forested areas to densely populated urban centers. Since the sampling design of our study does not lend itself to a formal analysis of spatial autocorrelation, we explored spatial patterns with DOM proxies in maps (Fig. 1b,c) but found no obvious relationships. Instead, type-specific characteristics of the water bodies were pronounced, largely independent of hydrological connections. Factors potentially contributing to the resulting heterogeneity across the surface waters in the city include specific local stressors such as point-source inputs of pollutants, spatially variable urban surface runoff delivering allochthonous DOM, and hydraulic-engineering structures such as sluices. Thus, our map of DOM composition (Fig. 1b,c) could be interpreted as visualizing ~~urban~~ heterogeneity in ~~aquatic ecosystem diversity and condition~~the conditions of urban surface freshwaters.

4.2 Seasonal patterns and drivers of DOM signatures

Seasonal variation in DOM signatures occurred in all types of water bodies mostly independent from variation among the four water body types. With a few exceptions, ~~P4 and~~ H3 being the most prominent ~~examples~~example, seasonal variation of DOM composition was consistent across all water body types. (Fig. 3a,b), Assessed separately at each site

(Fig. 3b), DOM was generally fresher in summer and autumn than in winter and spring, as indicated by higher ratios of β:α and more HMWS-N as indicators of polysaccharides and proteins (Thurman, 1985), whereas humic matter was more abundant in winter, and the pattern in spring was not clear-cut. Our rank-based analysis of PC2 scores (Fig. 3c) suggests a consistent seasonal pattern of changes in DOM composition across sites, which emerged even though the variation within individual sites was limited along PC2.

At least four potential processes could account for the observed seasonal turnover in DOM composition: exudates of aquatic primary producers, microbial and sunlight-induced transformation of DOM, and terrestrial inputs from riparian vegetation (Spencer et al., 2009; Cory et al., 2015), all of which could be influenced by the urban environment. Seasonal variation in light conditions could be important in influencing DOM composition by primary producers, independent of nutrient supply (see above), and temperature changes might also play a role, especially in determining rates of microbial DOM transformations. Pulses of leaf litter falling or swept or blown into urban water bodies could be an additional source of DOM varying with season (Gessner et al., 1999). This holds particularly for urban green spaces and water courses lined by woody riparian vegetation. However, quantification of the relative importance of different drivers of seasonal patterns remains difficult based on the data currently available for urban settings.

The ponds and streams included in our study showed higher and less predictable seasonal ~~turnover~~changes in DOM composition than the lakes and rivers, as revealed by the pattern along PC2 (Fig. 3). This ~~indicates~~indicates that the nature and degree of aquatic-terrestrial coupling in urban settings leaves an imprint on seasonal changes in DOM composition. Therefore, the ~~turnover of DOM. Surveys~~more extensive the time series data from surveys of DOM dynamics ~~should hence be more informative~~, the better can they inform about ecosystem conditions ~~than assessments based on single grab samples or averaged data.~~, complementing established procedures in water quality assessment and monitoring. ~~Inputs of DOM from WWTP effluents may also be captured by the seasonal patterns, although that influence is likely variable, as indicated by considerable seasonal turnover of DOM at site H3contrasting with a minimal turnover at sites S5 and R7 (small ellipses in Fig. 3b), despite the influence of WWTP effluents at those sites~~.

4.3 DOM composition as a potential basis for urban surface water monitoring

The fact that our analysis of DOM composition revealed ~~behavior~~specific characteristics of individual water bodies underlines the potential ~~usefulness~~value of DOM descriptors as ~~ecosystem-scale functional~~ indicators that could be included in ~~regular~~ water-quality assessment and monitoring. Some sites deviated from the general pattern observed for water bodies of the same type. P4, for example, was formerly connected to an ~~sewage farm~~old waste water treatment plant and appeared to be influenced by previously unrecognized ~~storm water~~stormwater runoff ~~that likely delivered inputs during heavy rain. The site was characterized by~~. This legacy matches the particularly high levels of nutrients characterizing this site, especially NH_4^+, ~~and~~combined with a distinct DOM composition. Similarly, S5, located immediately downstream of a WWTP, although not specifically selected as a highly polluted site, also showed a distinct DOM composition as reflected by its highly negative PC1 score (Fig. 2a), indicating that the allochthonous influence was likely the strongest among all sites. Site R7 showed the same pattern as S5, and although not initially recognized as being affected by a WWTP, its DOM composition revealed that it had ~~actually received WWTP effluents, which happened since the end 2015 (Nega et al., 2019).~~received WWTP effluents, which has actually

happened since the end of 2015 (Nega et al., 2019). The distinct signatures at these individual sites are thus a promising starting point for incorporating information on DOM composition in water-quality assessment and monitoring. ~~Notably,~~ DOM optical indic~~ex~~es ~~are~~would be highly cost-effective to apply and yield information that is not easily obtained by classic approaches. Robustness of such assessments would further increase when they are based on continuous time series. This could strengthen the implementation of current legal frameworks such as the EU Water Framework Directive aiming at an integrative water-quality assessment, including of urban water bodies.

5. Conclusion

The composition of DOM ~~collected~~analyzed in a suite of contrasting water bodies ~~in~~of a large metropolitan area, the city of Berlin in Germany, is diverse~~,~~. ~~varying~~ varying widely in molecular size and other features related to the degree of allochthonous inputs and conveying a distinct urban character. DOM features clearly differentiated water body types, from lakes with highly abundant autochthonous DOM to streams with more allochthonous DOM. Seasonal variation of DOM was prevalent in all water body types but likely to be driven not only by phenology but also by ~~distinctly~~ urban ~~drivers~~influences such as nutrient supply, WWTP ~~inputs~~ effluents, reduced leaf litter input or flashy runoff resulting from sealed surfaces. Nutrient supply, the percentage of green space and concentrations of trace organic pollutants (as proxies for point source influences) were identified as ~~major~~ drivers of DOM composition. ~~Notably, easily measured~~In particular, simple optical ~~data on DOM~~measurements of DOM characteristics were sufficient to detect WWTP effluents, a result that was ~~confirmed~~corroborated by our data on ~~TrOC~~TrOCs. This suggests that optical analysis of DOM ~~analyses~~ could be a useful ~~starting point in~~approach to complement current water-quality assessments and monitoring. ~~Optical~~ Such analyses ~~of DOM~~ are fast, inexpensive and easily implemented, and could be ~~complemented~~further supported by more sophisticated ~~and~~, potentially automated analyses such as the mass-spectrometric quantification of TrOCs. DOM composition can inform about processes both within water bodies and in the terrestrial surroundings~~,~~; therefore, water-quality assessments could benefit from integrating information on DOM composition. Robustness of the ~~assessments~~approach would increase if the DOM assessments were based on time series or even continuous monitoring, for which knowledge and technology ~~for which~~ are ~~readily~~already available~~.~~ ~~This could~~; this could~~,~~ indeed ~~and thus~~ strengthen ~~current~~ assessments as implemented in legal frameworks such as the EU Water Framework Directive~~, which aims at an integrative assessment of the "ecological status" of water bodies.~~

.

Appendix A includes a table showing site coordinates land cover and special features

Table A1: Coordinates, land cover, origin and special features. Longitude is given in decimal degrees East and latitude in decimal degrees North.

Site ID	Site name	Water body type	Latitude	Longitude	Agri-culture (%)	Forest (%)	Urban pave-ment (%)	Urban green space (%)	Origin
H1	Teltowkanal	River	52.44239	13.32454	0	0	60	30	Artificial
H2	Teltowkanal	River	52.42642	13.52039	0	0	100	0	Artificial
H3	Wuhle	Stream	52.52562	13.57913	50	0	50	0	Natural
H4	Tegeler Fliess	Stream	52.63442	13.38013	50	0	10	40	Natural
L1	Biesdorfer See	Lake	52.50331	13.5497	0	0	50	50	Artificial
L2	Obersee	Lake	52.54856	13.48972	0	0	50	50	Artificial
L3	Ploetzensee	Lake	52.5438	13.33049	0	0	0	100	Natural
L4	Gross Glienicker	Lake	52.46417	13.11489	0	10	0	90	Natural
L5	Havel	Lake	52.4431	13.14453	0	0	100	0	Natural
L6	Schlachtensee	Lake	52.44066	13.21183	0	60	30	10	Natural
L7	Müggelsee	Lake	52.43837	13.6451	0	70	30	0	Natural
P1	Hoheheideteich	Pond	52.57694	13.16428	0	100	0	0	Natural
P2	Hamburger Teich	Pond	52.56738	13.44549	0	0	30	70	Artificial
P3	Ruhwaldteich	Pond	52.52573	13.25998	0	0	50	50	Artificial
P4	Kienhorstbecken	Pond	52.57724	13.34556	0	0	0	100	Artificial
P5	Mittelfeldteich	Pond	52.61208	13.23045	0	100	0	0	Artificial
P6	Neurandteich	Pond	52.63883	13.27377	0	0	65	35	Artificial
P7	Möwensee	Pond	52.55282	13.33545	0	0	30	70	Artificial

R1	Müggelspree	River	52.42985	13.68912	0	0	100	0	Natural
R2	Landwehrkanal	River	52.51935	13.31959	0	0	80	20	Artificial
R3	Spree	River	52.53613	13.21622	0	0	100	0	Natural
R4	Kuhlake	River	52.57817	13.16509	0	100	0	0	Natural
R5	Neukölln Canal	River	52.48936	13.43949	0	0	30	70	Artificial
R6	Spree	River	52.47137	13.49683	0	0	100	0	Natural
R7	Panke	River	52.5369	13.36759	0	0	60	40	Natural
S1	Zingergraben	Stream	52.58209	13.38594	0	0	95	5	Artificial
S2	Schwarzer Graben	Stream	52.56488	13.34918	0	0	50	50	Natural
S3	Graben 1 Buch	Stream	52.62384	13.46883	0	100	0	0	Artificial
S4	Graben 73 Buchholz	Stream	52.62881	13.45315	100	0	0	0	Artificial
S5	Erpe	Stream	52.45888	13.61245	0	50	50	0	Natural
S6	Koppelgraben	Stream	52.62065	13.41089	50	0	30	20	Unknown
S7	Plumpengraben	Stream	52.41513	13.5628	0	0	100	0	Natural

525

Appendix B includes tables that complement the physico-chemical and dissolved organic composition information.

Table A1B1: Physico-chemical characteristics (mean ± SD and % variance explained) of four contrasting types of water bodies in the city of Berlin. Means and standard deviations were computed across all seasons and sites. The percentages of variance explained (% Var) refer to the effect of season within each water body type, calculated by type-II ANOVA (aka variance component analysis), with season treated as a random factor. F-values refer to results of repeated-measures ANOVAs testing for differences among water body types (* p<0.001, * p<0.05, ns = not significant).**

Water body	Temperature		DOC		TP		NH_4^+		NO_3^-		Chlorophyll *a*	
type	(°C)	% Var	(mg/L)	% Var	(mg/L)	% Var	(mg/L)	% Var	(mg/L)	% Var	(µg/L)	% Var
Lakes	14.6 ± 6.9	94	7.5 ± 2.7	23	0.05 ± 0.05	34	0.07 ± 0.07	26	0.22 ± 0.36	48	6.2 ± 14.2	61
Ponds	13.7 ± 5.3	94	10.3 ± 3.0	32	0.09 ± 0.07	30	0.27 ± 0.67	30	0.03 ± 0.06	52	7.3 ± 7.7	55
Rivers	15.2 ± 6.2	92	8.0 ± 1.6	13	0.10 ± 0.08	43	0.15 ± 0.14	68	1.12 ± 1.66	46	2.1 ±2.9	51
Streams	11.3 ± 4.9	87	11.7 ± 5.5	42	0.26 ± 0.31	21	0.36 ± 0.65	76	0.91 ± 1.53	43	5.3 ± 9.7	53
$F_{water\ body}$	9.4***		3.8*		2.8^{ns}		1.3^{ns}		2.5^{ns}		1.0^{ns}	

Table ~~A2: Absorbance~~B2: Description of absorbance and ~~Fluorescence~~fluorescence indices ~~definition~~.

Variable	~~Definition~~Description
$SUVA_{254}$	Proxy for DOM aromaticity (Weishaar et al., 2003)
E2:E3	Ratio of absorbance at 250 and 365 nm, as an (inverse) indicator of molecular size (Peuravuori and Pihlaja, 1997) (Chen et al., 1977)
E4:E6	Indicator of humification (Chen et al., 1977)
~~Slope short~~SR	~~Short wavelength slope within the wavelength region of 275-295 nm as an inverse correlate with molecular weight and aromaticity (Helms et al., 2008)~~Ratio of slopes (SR) computed from short and long wavelength regions as another negative correlate with DOM molecular weight (Loiselle et al., 2009)
~~SR~~FI	~~Ratio of slopes (SR) computed from short and long wavelength regions as another negative correlate with DOM molecular weight (Loiselle et al., 2009)~~Fluorescence index (FI) Ratio of the fluorescence intensities at the emissions 470 and 520 (obtained at excitation wavelength of 370nm). Indicator of DOM derived from terrestrial plants (FI around 1.2) or from microbes or algae (FI around 1.4) (Fellman et al., 2010; Cory and Mcknight, 2005; Cory et al., 2010; Jaffé et al., 2008)
~~FIX~~ HIX	~~Fluorescence index (FIX) as the ratio of fluorescence intensities at the emission wavelengths of 470 and 520 nm (obtained at excitation wavelength of 370 nm), which has proved useful to distinguish the relative contributions of terrestrial (FIX~1.4) and aquatic (FIX~1.9) sources of DOM (Mcknight et al., 2001)~~Humification index (HIX) as a proxy for humic substances (Ohno, 2002)
~~HIX~~β/α	~~Humification index (HIX) as a proxy for humic substances (Ohno, 2002)~~Freshness index β/α (Wilson and Xenopoulos, 2009), which indicates the relative importance of recently produced DOM (Parlanti et al., 2000)
~~β/α~~	~~Freshness index β/α (Wilson and Xenopoulos, 2009), which indicates the relative importance of recently produced DOM (Parlanti et al., 2000)~~

Table ~~A3~~B3: Designation, excitation (Ex) and emission (Em) wavelengths of PARAFAC components, and the number of studies with matching components reported in OpenFluor (checked on the 28th March 2022) (Murphy et al., 2014).

PARAFAC component	Ex	Em	OpenFluor reference matches (0.95)	Explanation and selected references
C1	250	446	12~~8~~	Humic-like, peak A (Coble, 1996); humic-like and recalcitrant (C1) (Hansen et al., 2016)
C2	250	500	70~~22~~	Terrestial humic-like in waste water treatment impacted water, (G1) (Murphy et al., 2011); ubiquitous and recalcitrant humic (C2) (Chen et al., 2017)
C3	306	408	20~~13~~	Humic-like, peak M (Coble, 1996); humic-like (C3) (Stedmon and Markager, 2005)
C4	256	444	8~~9~~	Terrestrial humic-like, suggested as photo-refractory (C2) (Yamashita et al., 2010); terrestrial humic-like (C3) (Williams et al., 2013)
C5	250	382	12~~2~~	Anthropogenic, microbial humic-like (C6) (Williams et al., 2016)
C6	294	352	33~~13~~	Similar to tryptophan (C3) (Catalán et al., 2015); protein-like, linked to autochthonous production (C3) (Amaral et al., 2016)
~~C7~~	~~320~~	~~396~~	~~8~~	~~Humic-like, peak M (Coble, 1996); microbially transformed autochthonous DOM (C2) (Osburn et al., 2011)~~
C7~~8~~	276	326	68~~15~~	Protein-like, peak B (Coble, 1996); waste water treatment protein (C2) (Teymouri, 2007)

Table ~~A4: Absorbance~~B4: Variables of absorbance and fluorescence ~~analysis variables~~analyses (mean ± SD and % variance explained) in contrasting types of urban surface ~~water body~~waters. Means and standard deviations were computed across all seasons and sites. The percentages of variance explained (% Var) refer to the effect of season within each water body type, calculated by a type-II ANOVA (aka variance component analysis), with season treated as a random factor. F-values refer to results of repeated-measures ANOVA testing for differences among water body types (*p<0.001, **p<0.01, *p<0.05, ns = not significant). Abbreviations explained in Table ~~A2~~B2.**

Water body type	$SUVA_{254}$		E2:E3		E4:E6		~~Slope short~~		SR		FI~~X~~		HIX		β/α	
		% Var		% Var		% Var	-	~~% Var~~		% Var		% Var		% Var		% Var
Lakes	1.55 ± 0.39	20	8.99 ± 2.14	6	3.02± 1.34	67	~~-0.024 ± 0.004~~	~~8~~	1.38 ± 0.27	12	1.61 ± 0.08	69	0.77 ± 0.08	9	0.86 ± 0.09	12
Ponds	2.14 ± 0.51	37	6.65 ± 1.24	14	3.12± 0.74	46	~~-0.019 ± 0.003~~	~~13~~	1.20 ± 0.19	29	1.52 ± 0.06	61	0.83 ± 0.04	47	0.70 ± 0.04	35
Rivers	2.25 ± 0.15	55	7.04 ± 0.98	12	4.40± 14.27	80	~~-0.019 ± 0.002~~	~~22~~	0.017 ± 0.002	76	0.68 ±0.11	10	0.85 ± 0.03	24	0.79 ± 0.09	19
Streams	2.50 ±0.52	65	6.328 ± 0.876	54	3.53± 2.31	75	~~-0.017 ± 0.001~~	~~57~~	0.97 ± 0.13	22	1.63 ± 0.14	11	0.86 ± 0.05	21	0.73 ± 0.10	24
$F_{water\ body}$	11.8***		5.8**		2.6 ^{ns}		~~8.0***~~	-	9.2***		3.5*		4.9**		5.5**	

Table A5B5: PARAFAC components results (mean ± SD and % variance explained) in contrasting types of urban surface water bodywaters. Means and standard deviations were computed across all seasons and sites. The percentages of variance explained (% Var) refer to the effect of season within each water body type, calculated by a type-II ANOVA (aka variance component analysis), with season treated as a random factor. F-values refer to results of repeated-measures ANOVA testing for differences among water body types (*p<0.001, **p<0.01, *p<0.05, ns = not significant).**

Water body type	C1	% Var	C2	% Var	C3	% Var	C4	% Var	C5	% Var	C6	% Var	C7	% Var	C8	% Var
Lakes	0.17 ± 0.09	20	0.12 ± 0.06	14	0.17 ± 0.08	27	0.23 ± 0.10	11	0.23 ± 0.16	10	0.20 ± 0.10	15	0.09 ± 0.05	27	0.17 ± 0.10	9
Ponds	0.27 ± 0.07	60	0.22 ± 0.09	65	0.34 ± 0.17	57	0.32 ± 0.15	48	0.36 ± 0.29	37	0.16 ± 0.07	54	0.08 ± 0.05	67	0.22 ± 0.11	48
Rivers	0.59 ± 0.41	8	0.34 ± 0.17	12	0.28 ± 0.10	56	0.37 ± 0.09	38	0.42 ± 0.19	41	0.35 ± 0.25	12	0.37 ± 0.33	7	0.23 ± 0.12	15
Streams	0.88 ± 0.55	18	0.56 ± 0.29	32	0.55 ± 0.48	65	0.67 ± 0.47	44	0.82 ± 0.62	64	0.42 ± 0.32	24	0.46 ± 0.43	16	0.33 ± 0.17	47
$F_{water\ body}$	6.7***	-	10.5***	-	7.4***	-	6.8***	-	8.0***	-	2.7^{ns}	-	3.8*	-	$2.8^{n.s.}$	-

Water body type	C1	% Var	C2	% Var	C3	% Var	C4	% Var	C5	% Var	C6	% Var	C7	% Var
Lakes	0.17 ± 0.10	17	0.13 ± 0.06	14	0.24 ± 0.12	20	0.28 ± 0.12	14	0.31 ± 0.18	11	0.19 ± 0.10	15	0.18 ± 0.11	9
Ponds	0.24 ± 0.14	73	0.24 ± 0.11	80	0.40 ± 0.22	63	0.46 ± 0.21	63	0.52 ± 0.38	73	0.16 ± 0.11	65	0.25 ± 0.14	45
Rivers	0.51 ± 0.34	8	0.34 ± 0.17	12	0.66 ± 0.37	10	0.44 ± 0.12	32	0.61 ± 0.26	30	0.32 ± 0.22	14	0.25 ± 0.14	14
Streams	0.76 ± 0.47	16	0.57 ± 0.30	53	1.00 ± 0.58	30	0.85 ± 0.63	64	1.08 ± 0.73	16	0.37 ± 0.29	25	0.35 ± 0.18	45
Fwater body	6.3**		10.4***		7.6***		7.2***		8.4***		2.2n.s		2.6n.s.	

Table ~~A6: Size~~B6: Results of size exclusion chromatography ~~results~~ (mean ± SD and % variance explained) ~~in~~of samples from contrasting types of urban surface ~~water body~~waters. Means and standard deviations were computed across all seasons and sites. The percentages of variance explained (% Var) refer to the effect of season within each water body type, calculated by a type-II ANOVA (aka variance component analysis), with season treated as a random factor. F-values refer to results of repeated-measures ANOVA testing for differences among water body types (*p<0.001, **p<0.01, *p<0.05, ns = not significant). HS, humic-like substances; HMWS, high-molecular weight non-humic substances; and LMWS, low-molecular weight substances.**

Water body type	HMSW		HMSW		HS		HS		LMWS	
	(mg C/L)	% Var	(mg N/L)	% Var	(mg C/L)	% Var	(mg N/L)	% Var	(mg C/L)	% Var
Lakes	0.96 ± 0.74	27	0.11 ± 0.07	9	4.14 ± 1.49	19	0.25 ± 0.11	12	0.83 ± 0.26	18
Ponds	1.32 ± 0.60	41	0.16 ± 0.06	36	6.29 ± 2.42	26	0.33 ± 0.13	17	1.19 ± 0.46	45
Rivers	0.59 ± 0.20	60	0.09 ± 0.03	24	5.21 ± 0.97	33	0.31 ± 0.09	31	1.10 ± 0.41	22
Streams	0.73 ± 0.45	52	0.10 ± 0.05	41	7.21 ± 3.75	25	0.41 ± 0.27	9	1.48 ± 0.62	39
$\mathbf{F_{water\ body}}$	4.2*		2.9^{ns}		2.9^{ns}		$1.3^{ns.}$		3.7*	

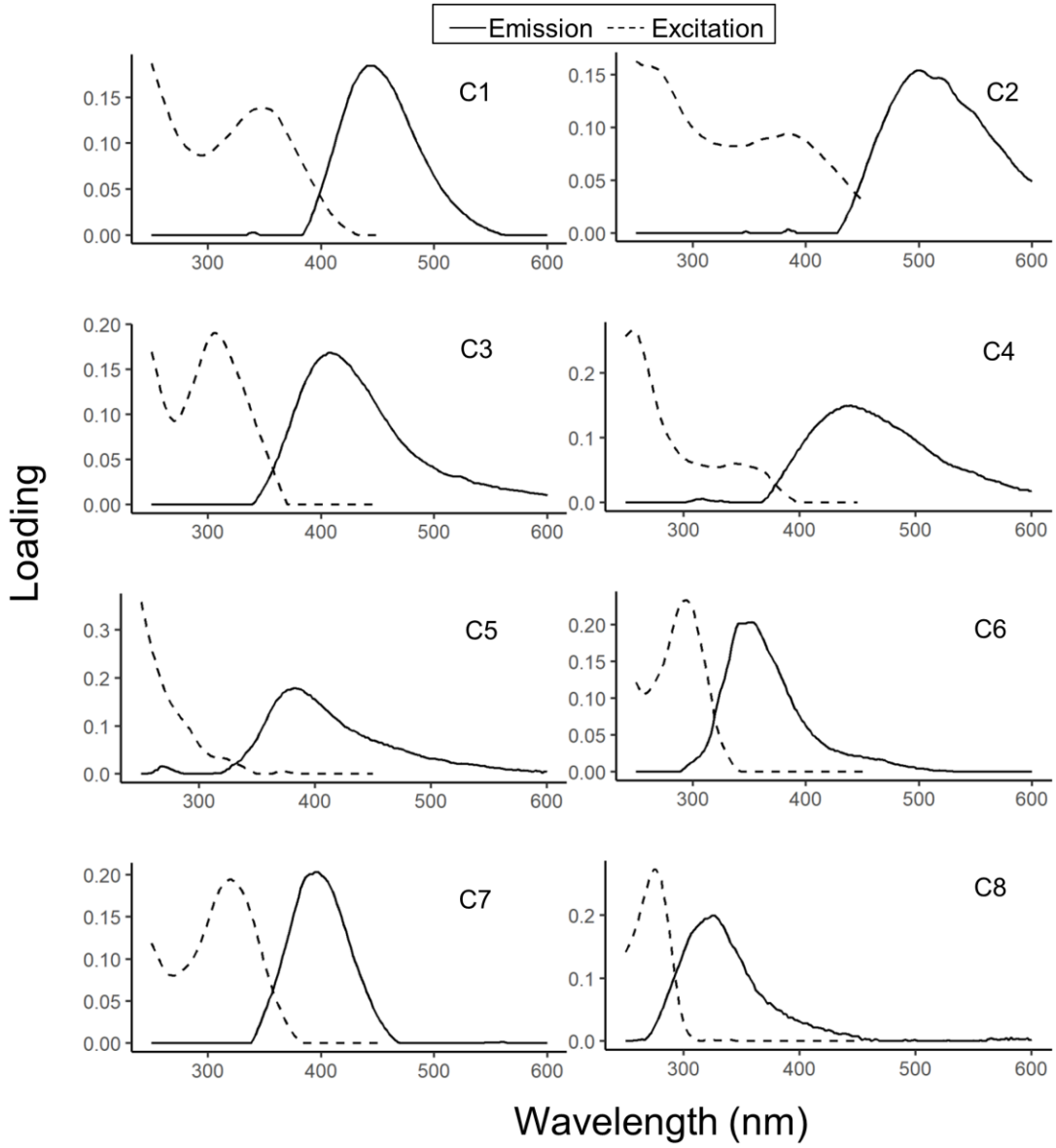

~~Figure A1 PARAFAC components emission and excitation wavelength.~~

575

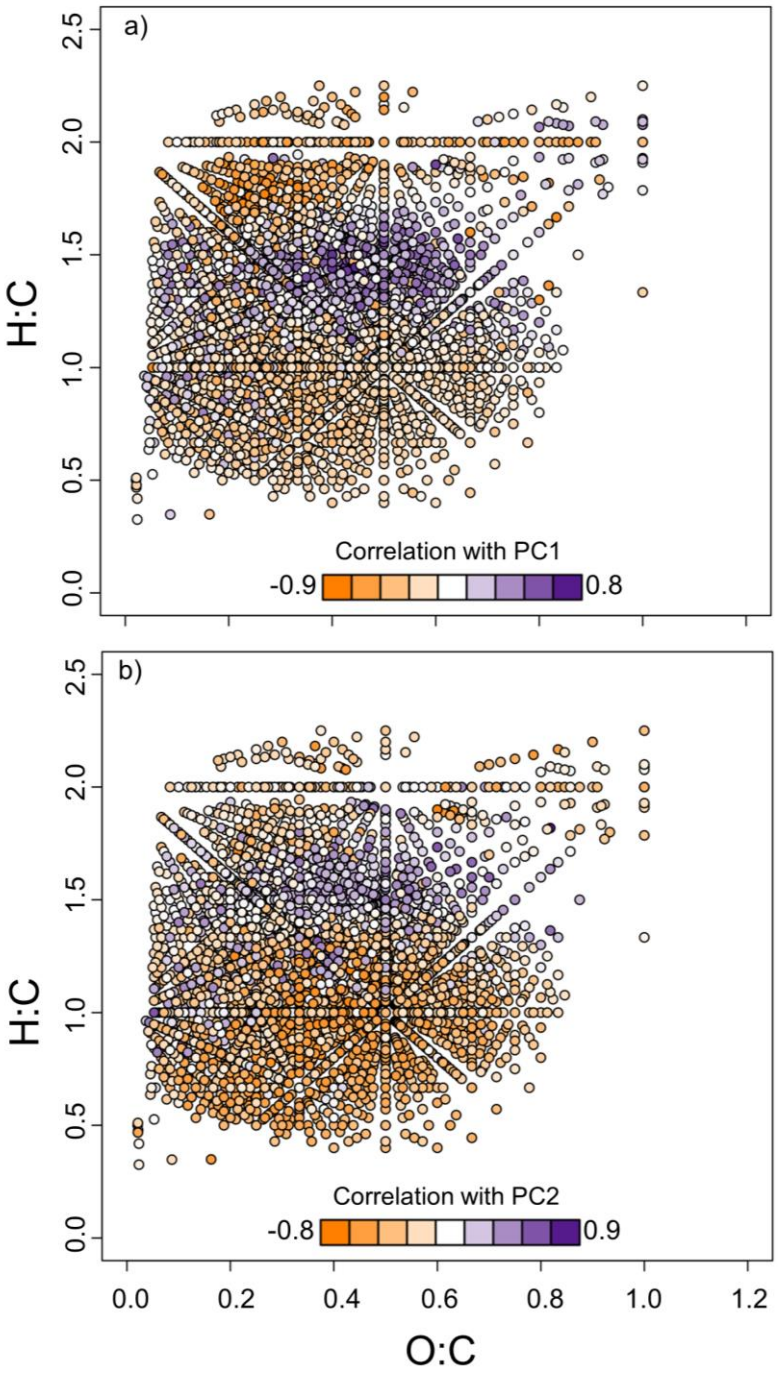
a)
H:C
0.0
0.5
1.0
1.5
2.0
2.5
Correlation with PC1
-0.9
0.8
b)
H:C
0.0
0.5
1.0
1.5
2.0
2.5
Correlation with PC2
-0.8
0.9
0.0
0.2
0.4
0.6
0.8
1.0
1.2
O:C

580

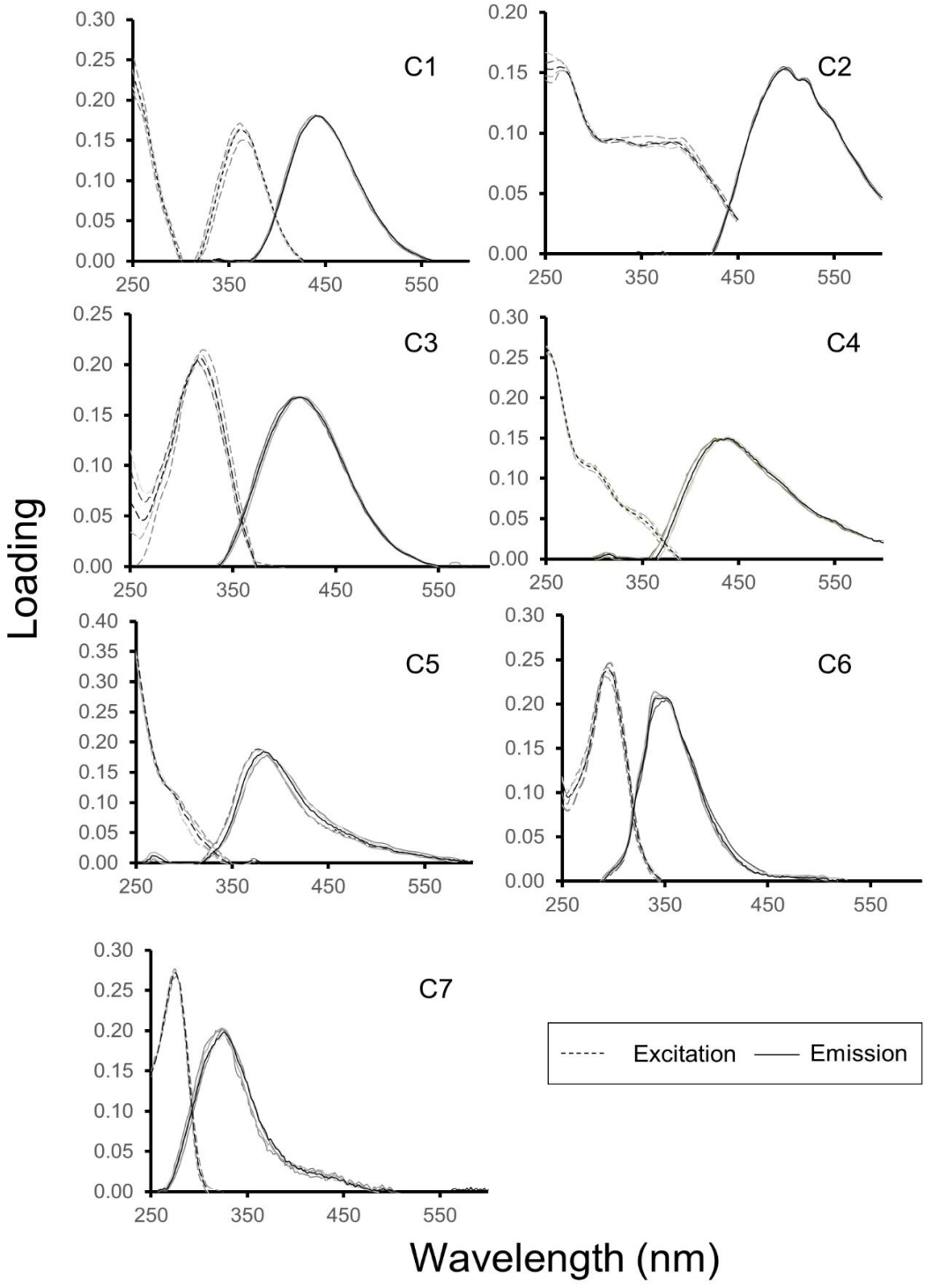

Figure B1 Emission and excitation wavelengths of PARAFAC components. Solid lines represent emission spectra, dashed lines excitation spectra. Lines in different shades of grey refer to models using different sample sub-sets of a split-half validation analysis.

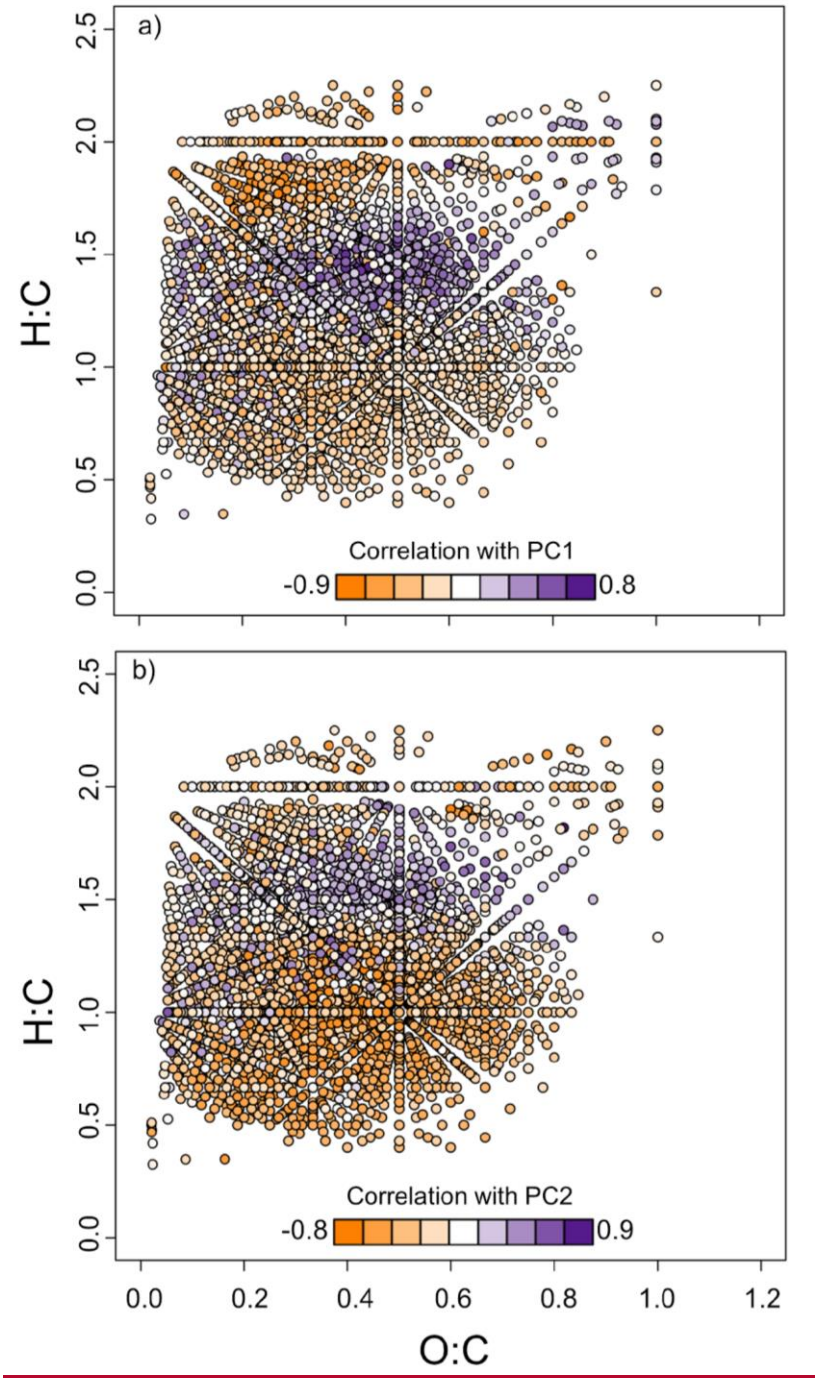

Figure ~~A2~~B2 Van Krevelen plots showing all molecules (sum formulas) identified by FT-ICR-MS analysis of DOM samples collected at 32 urban sites over three seasons (summer, autumn and winter). ~~Color~~Colour indicates molecule-specific Spearman correlation coefficients of the relative intensities of each compound with the first (a) and second (b) axis of the PCA shown in Figures 2 and 3. The data points were plotted in random order to avoid bias resulting from identical O:C and H:C ratios for many sum formulas.

Appendix ~~B~~C includes tables and figures that complement Trace Organic Compounds analysis

Table ~~B1~~C1: Trace organic compounds (TrOCs) analyzed in samples collected in urban surface waters. LLoQ = Limit of Quantification. Frequency refers to the number of occasions where concentrations exceeded the LLoQ.

Acronym	LLoQ (µg/L)	Frequency	Name	Description
ACS	0.1	72	Acesulfame	Sweetener
ATS	0.05	42	Amidrotrizoic	Radiocontrast agent
BTA	0.1	68	Benzotriazole	Corrosion inhibitor
BZF	0.1	6	Benzafibrate	Lipid-lowering agent
CBZ	0.05	44	Carbamazepine	Anticonvulsant
DCF	0.05	30	Diclofenac	Analgesic/anti-inflammatory agent
FAA	0.1	46	4-formylamin metabolite of metamizol	Analgesic
GAB	0.1	62	Gabapentin	Drug for epilepsy treatment/pain killer
GPL	0.05	39	Gabapentin-lactam	Derivate of gabapentin
IOM	0.1	40	Iomeprol	Radiocontrast agent
IOP	0.01	52	Iopromide	Radiocontrast agent
MBT	0.1	63	Methylbenzotriazole	Corrosion inhibitor
MTP	0.1	31	Metoprolol	Beta blocker
PRI	0.05	31	Primidone	Anticonvulsant
SMX	0.1	2	Sulfamethoxazole	Antibiotic
VAL	0.1	30	Valsartan	At1-receptor antagonist
VLX	0.1	3	Venlafaxine	Antidepressant
VSA	0.1	62	Valsartan acid	Antihypertensive agent

600 **Table ~~B2~~C2: Mean concentrations and standard deviations of Trace Organic Compound (TrOC) per water body type. See Table ~~B1~~C1 for full names. BZF, SMX and VLX were always below the limit of quantification (LLoQ) and are hence omitted from the table.**

	TrOC concentration (µg/L)			
Acronym	**Lakes**	**Ponds**	**Rivers**	**Streams**
ACS	0.23 ± 0.17	0.15 ± 0.16	0.28 ± 0.17	0.78 ± 1.35
ATS	0.08 ± 0.12	<LLoQ	0.74 ± 1.12	0.43 ± 0.88
BTA	0.34 ± 0.51	0.38 ± 0.91	2.37 ± 3.31	2.16 ± 3.61
CBZ	0.07 ± 0.08	<LLoQ	0.37 ± 0.48	0.41 ± 0.66
DCF	<LLoQ	<LLoQ	0.97 ± 1.38	0.88 ± 2.14
FAA	0.15 ± 0.23	<LLoQ	1.25 ± 1.66	2.10 ± 4.25
GAB	0.27 ± 0.36	<LLoQ	0.42 ± 0.43	0.74 ± 1.12
GPL	0.10 ± 0.17	<LLoQ	0.19 ± 0.42	0.13 ± 0.18
IOM	0.18 ± 0.28	<LLoQ	1.18 ± 2.36	1.44 ± 2.91
IOP	0.09 ± 0.19	0.01 ± 0.02	0.27 ± 0.32	1.46 ± 3.79
MBT	0.27 ± 0.39	0.11 ± 0.24	0.91 ± 1.01	0.69 ± 1.27
MTP	<LLoQ	<LLoQ	0.47 ± 0.58	0.63 ± 1.55
PRI	0.03 ± 0.02	<LLoQ	0.16 ± 0.22	0.26 ± 0.52
VAL	<LLoQ	<LLoQ	0.39 ± 0.44	0.97 ± 3.65
VSA	0.70 ± 1.02	<LLoQ	3.22 ± 3.84	3.33 ± 5.72

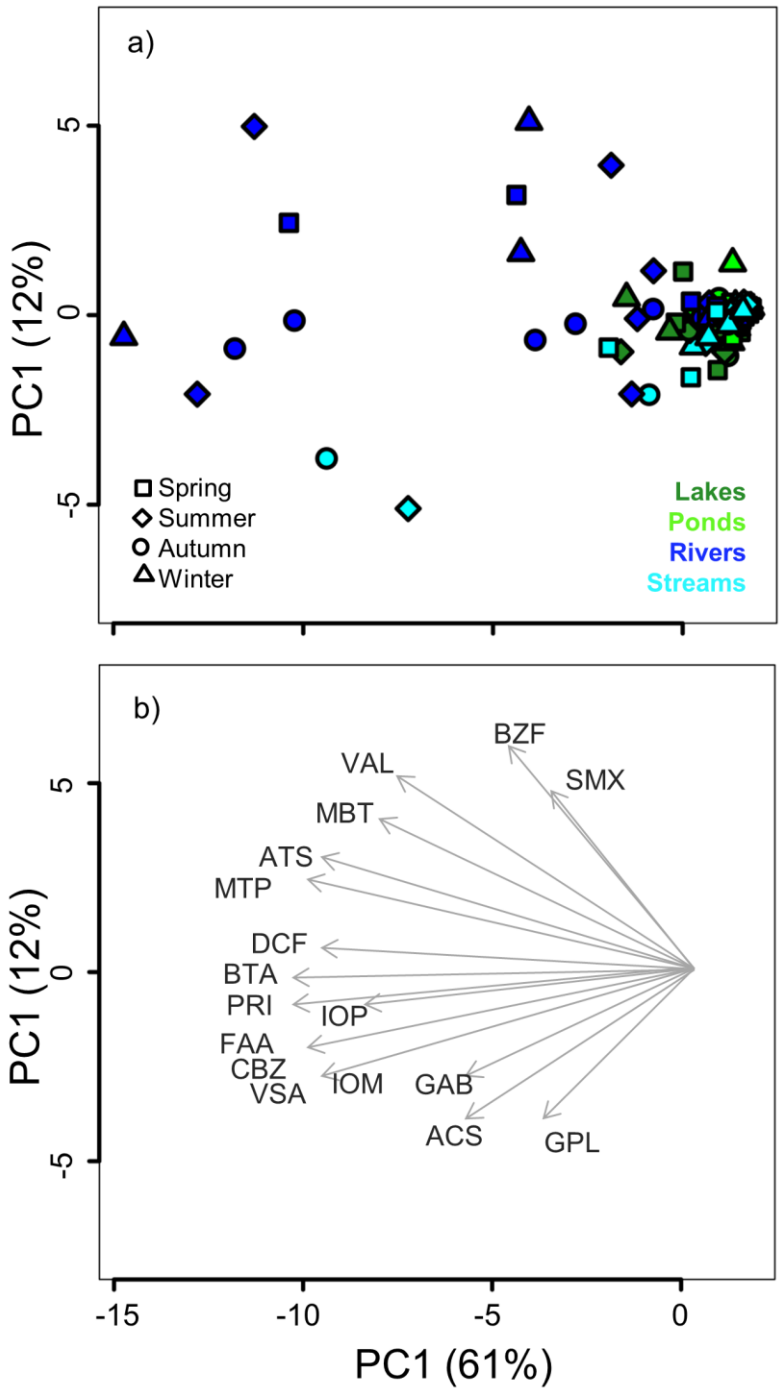
a)
PC1 (12%)
5
0
-5
Spring
Summer
Autumn
Winter
Lakes
Ponds
Rivers
Streams
b)
BZF
VAL
SMX
MBT
ATS
MTP
DCF
BTA
PRI
IOP
FAA
CBZ
VSA
IOM
GAB
ACS
GPL
-15
-10
-5
0
PC1 (61%)

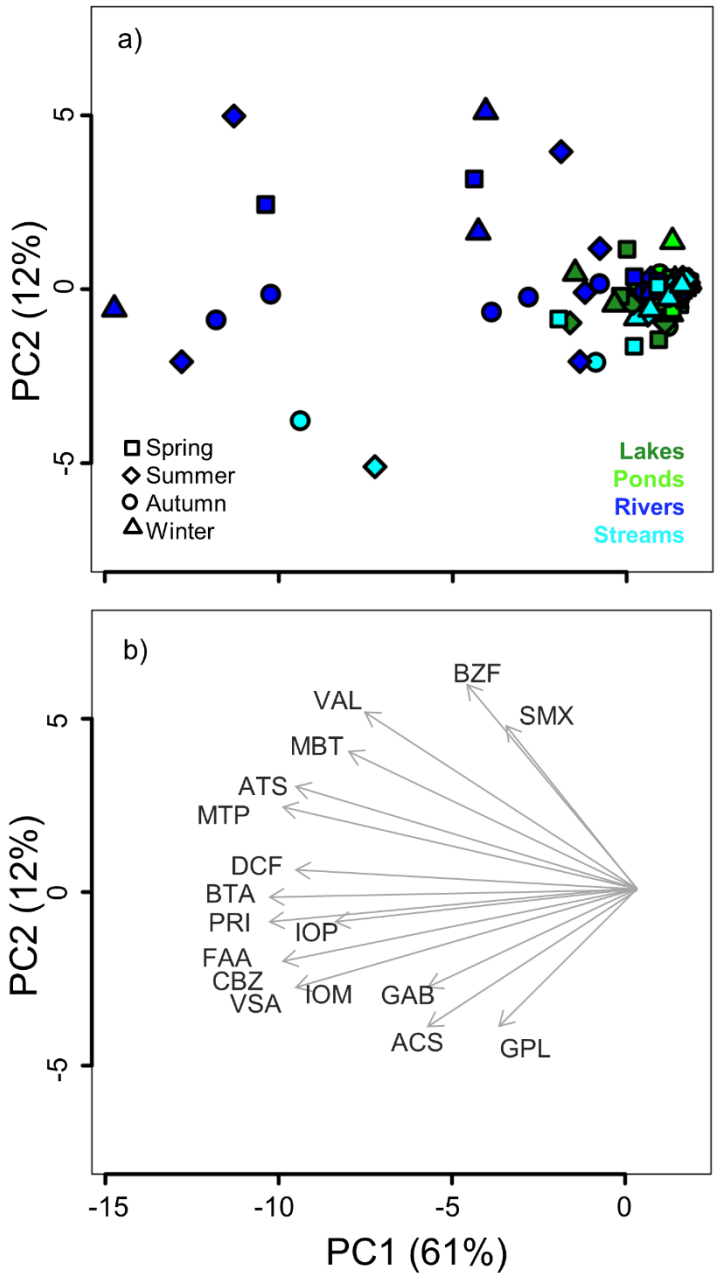

605

Figure ~~B1~~C1 Principal Component Analysis (PCA) of 32 urban ~~sampling~~ sites in the city of Berlin over four seasons (a) and Trace Organic Compounds (TrOCs) (b). ~~Extreme~~Site S5 had extreme PC1 and PC2 scores; the site ~~S5~~ was included in the analysis but is not presented in the biplot to better visualize variability among the other sites. Abbreviations of the TrOCs (B) are explained in Table ~~B1~~C1.

610

Appendix ~~C~~ D includes ~~figures that complement~~ the ~~statistical~~RDA analysis

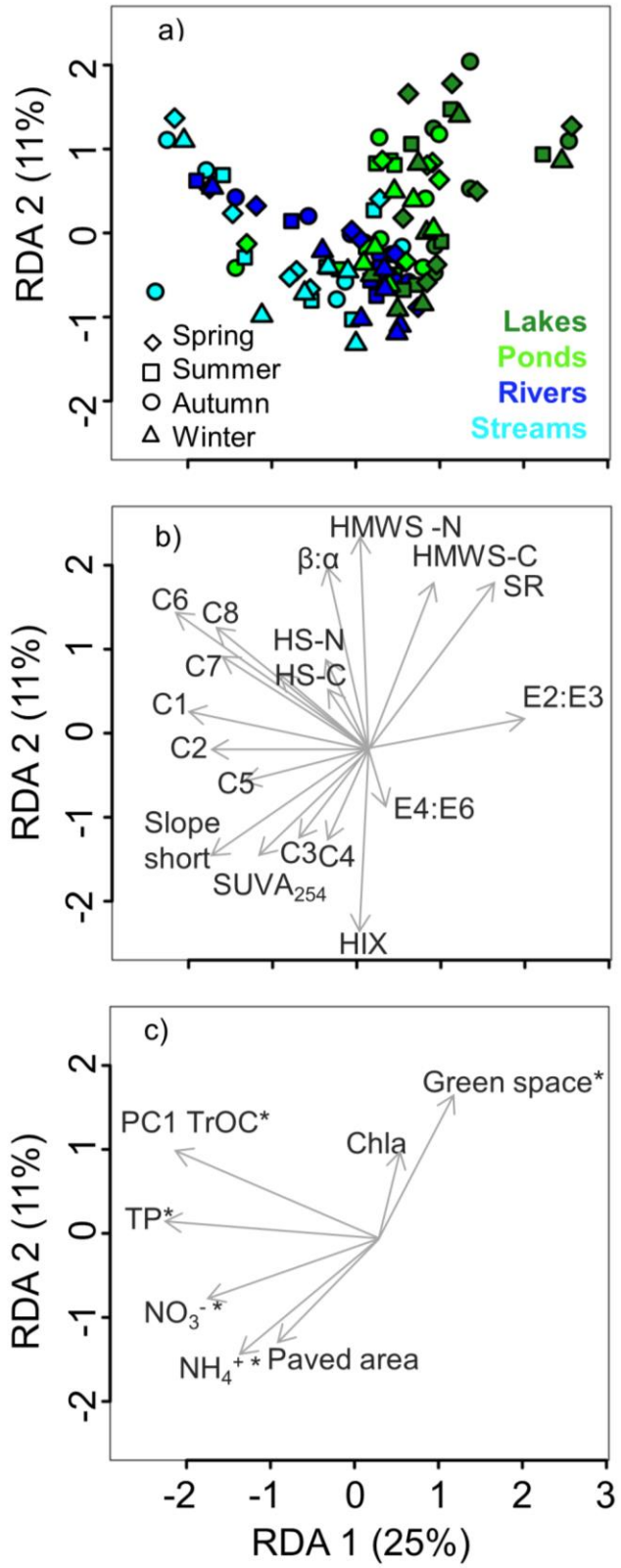

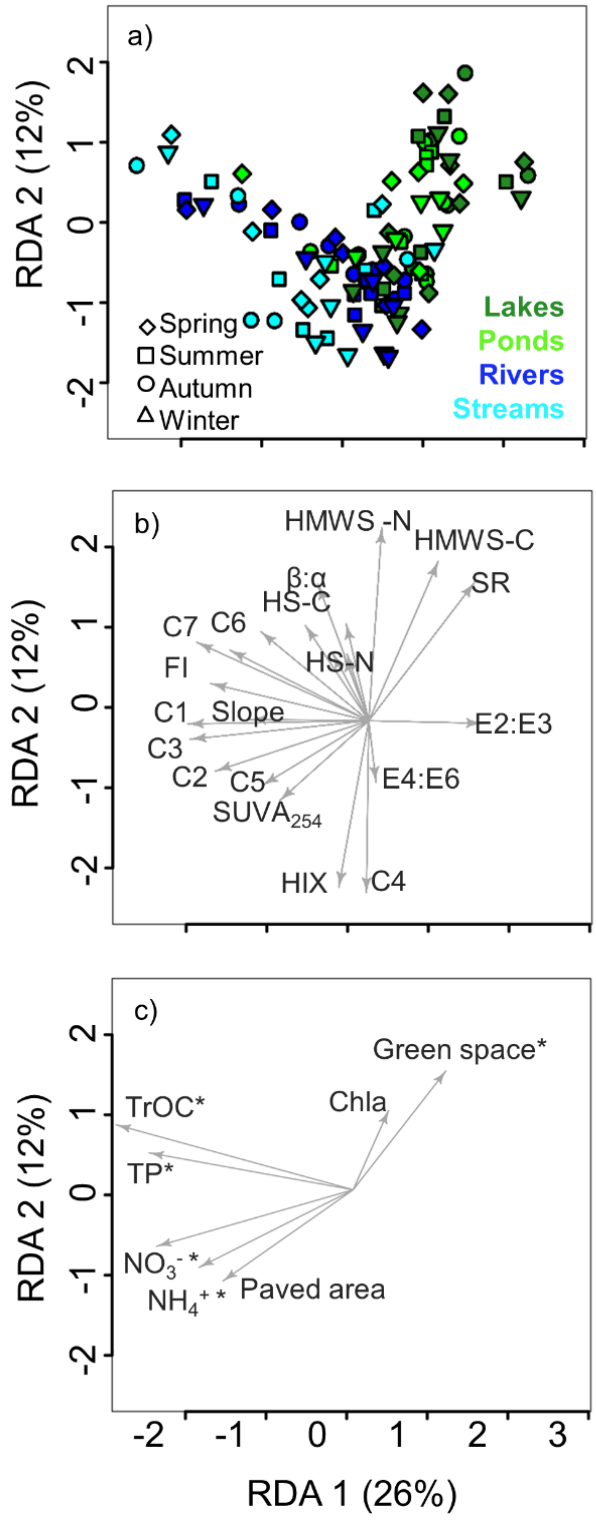

Figure ~~C1~~D1 Redundancy Analysis (RDA) of urban sampling sites (a) visited 4 times over one year, the DOM characteristics included in the analysis (b) and the predictor variables (c), the last marked by an asterisk (*) when significant. DOM characteristics include (i) absorbance and fluorescence indexes (E2:E3, molecular size, E4:E6, indicator of humification, SR, slope ratio, β:α, freshness index, ~~slope short,~~ $SUVA_{254}$ and HIX, humification index), (ii) PARAFAC components (C1 to

~~C8~~C7), and (iii) fractions derived from size exclusion chromatography (HS, humic-like substances; HMWS, high-molecular weight non-humic substances; and LMWS, low-molecular weight substances).

620

~~*Supplement.* The supplement related to this article is available online.~~**Appendix E Includes precipitation and flow in the city of Berlin during the study and the relation of Iron and absorbance at 420 relative to DOC.**

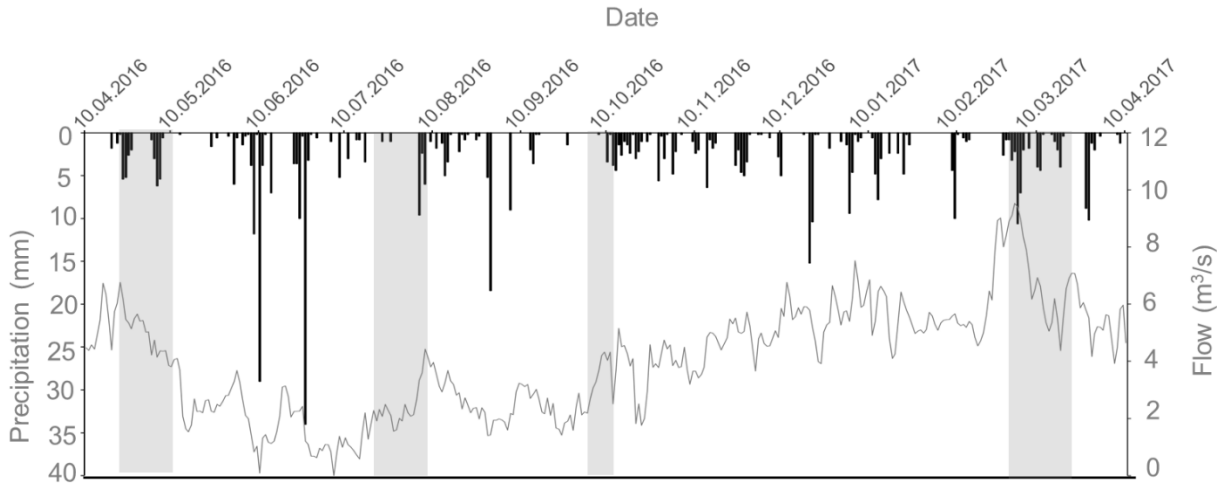

Figure E1 Precipitation and flow at a site within the city of Berlin during the study period, with the grey boxes indicating the four sampling periods.

625

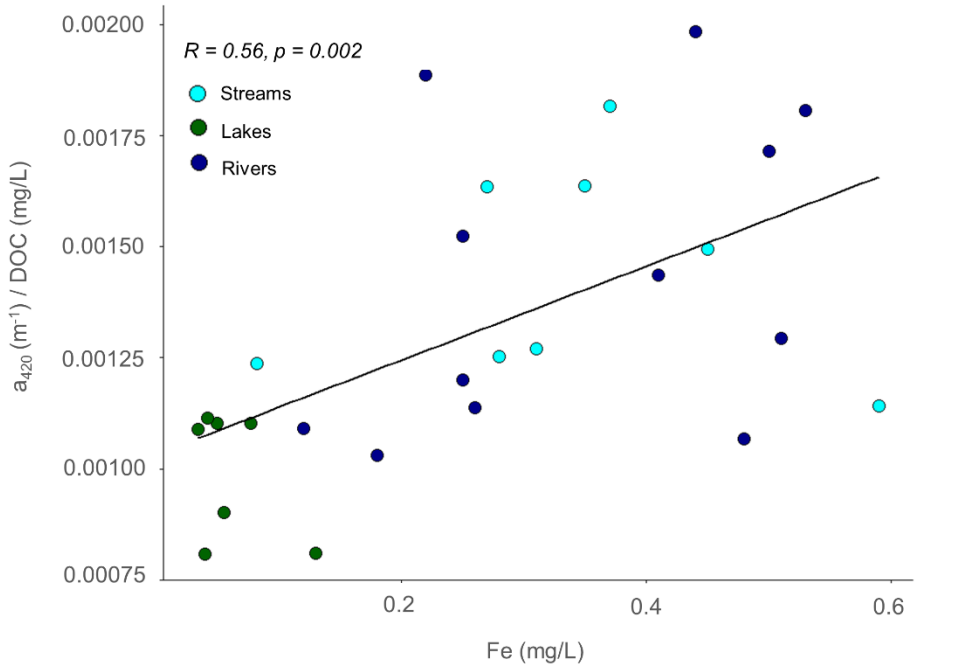

Figure E2 Relationship between iron (Fe) and the absorbance at 420nm relative to DOC(a420/DOC)

Author contributions. All authors contributed to designing the study. CR and SH collected the data. CR did the optical analysis and the PARAFAC model~~l~~ing, GS carried out the FT-ICR-MS analysis. CR and GS conducted the statistical analysis. CR led the manuscript writing, jointly with GS. All authors discussed results and edited the manuscript.

Competing interests. The authors declare ~~that they~~not to have ~~no~~a conflict of interest.

Data availability. The data will be made available at ~~a suitable repository at~~ ttps://www.pangaea.de/~~https://www.re3data.org/~~.

*Acknowledgments***.** We thank A. Köhler at the Senate Berlin (SenUVK) for water quality data, authorities and private land owners for providing access to the study sites, C.N. Stratmann for obtaining permissions, U. Mallok for nutrient analyses, C. Schmalsch for the LCOCD analysis, S. Krocker and T. Fuss for the DOC analysis and T. Goldhammer for advice with chemical analyses. C.N. Stratmann, Meinhold, I. Ajamil, G. Idoate, L. Thuile-Bistarelli, A. Sultan, R. Schulte, E. Tupper, T. Fuss, R. del Campo, A. Wieland, and M. Bethke for field assistance. G. Aschermann and A. Putschew kindly enabled TrOC analyses. Access to FT-ICR-MS and associated expertise was generously provided by T. Dittmar during a stay of G. Singer at the University of Oldenburg that was funded by the Hanse-Wissenschaftskolleg Delmenhorst. Thank you also to K. Pypkins for support with GIS and to B. Kleinschmit for ~~advice in~~thoughts on the sampling strategy and data analysis. This project was funded by the German Research Foundation (DFG) through the Research Training Group ‘Urban Water Interfaces’ (UWI; GRK 2032).

References

Amaral, V., Graeber, D., Calliari, D., and Alonso, C.: Strong linkages between DOM optical properties and main clades of aquatic bacteria, Limnology and Oceanography, 61, 906-918, 10.1002/lno.10258, 2016.

Baume, O. and Marcinek, J.: Das Berliner Gewässernetz und seine Nährstoffbelastung, Wasserwirtschaft Wassertechnik, , 6, 40-45 (In German), 1993

Bro, R.: PARAFAC. Tutorial and applications, Chemometrics and Intelligent Laboratory Systems, 38, 149-171, http://dx.doi.org/10.1016/S0169-7439(97)00032-4, 1997.

~~Buerge, I. J., Buser, H. R., Kahle, M., Müller, M. D., and Poiger, T.: Ubiquitous Occurrence of the Artificial Sweetener Acesulfame in the Aquatic Environment: An Ideal Chemical Marker of Domestic Wastewater in Groundwater, Environmental Science & Technology, 43, 4381-4385, 10.1021/es900126x, 2009.~~

Carpenter, S. R., Caraco, N. F., Correll, D. L., Howarth, R. W., Sharpley, A. N., and Smith, V. H.: Nonpoint pollution of surface waters with phosphorus and nitrogen, Ecological Applications, 8, 559-568, 10.1890/1051-0761(1998)008[0559:NPOSWW]2.0.CO;2, 1998.

Catalán, N., Obrador, B., Alomar, C., and Pretus, J. L.: Seasonality and landscape factors drive dissolved organic matter properties in Mediterranean ephemeral washes, Biogeochemistry, 112, 261-274, 10.1007/s10533-012-9723-2, 2013.

Catalán, N., Kellerman, A. M., Peter, H., Carmona, F., and Tranvik, L. J.: Absence of a priming effect on dissolved organic carbon degradation in lake water, Limnology and Oceanography, 60, 159-168, 10.1002/lno.10016, 2015.

Chen, H., Liao, Z.-l., Gu, X.-y., Xie, J.-q., Li, H.-z., and Zhang, J.: Anthropogenic Influences of Paved Runoff and Sanitary Sewage on the Dissolved Organic Matter Quality of Wet Weather Overflows: An Excitation–Emission Matrix Parallel Factor Analysis Assessment, Environmental Science & Technology, 51, 1157-1167, 10.1021/acs.est.6b03727, 2017.

Chen, Y., Senesi, N., and Schnitzer, M.: Information provided on humic substances by E4/E6 ratios, Soil Sci. Soc. Am. J. 41, 352–358., 1977.

Coble, P. G.: Characterization of marine and terrestrial DOM in seawater using excitation-emission matrix spectroscopy, Marine Chemistry, 51, 325-346, http://dx.doi.org/10.1016/0304-4203(95)00062-3, 1996.

Cory, R. M. and McKnight, D. M.: Fluorescence Spectroscopy Reveals Ubiquitous Presence of Oxidized and Reduced Quinones in Dissolved Organic Matter, Environmental Science & Technology, 39, 8142-8149, 10.1021/es0506962, 2005.

Cory, R. M., Harrold, K. H., Neilson, B. T., and Kling, G. W.: Controls on dissolved organic matter (DOM) degradation in a headwater stream: the influence of photochemical and hydrological conditions in determining light-limitation or substrate-limitation of photo-degradation, Biogeosciences, 12, 6669-6685, 10.5194/bg-12-6669-2015, 2015.

Cory, R. M., Miller, M. P., McKnight, D. M., Guerard, J. J., and Miller, P. L.: Effect of instrument-specific response on the analysis of fulvic acid fluorescence spectra, Limnology and Oceanography: Methods, 8, 67-78, https://doi.org/10.4319/lom.2010.8.67, 2010.

Cotton, J. B. and Scholes, I. R.: Benzotriazole and Related Compounds as Corrosion Inhibitors For Copper, British Corrosion Journal, 2, 1-5, 10.1179/000705967798327235, 1967.

Council, N. R.: Urban Stormwater Management in the United States. Washington, DC: The National Academies Press. https://doi.org/10.17226/12465., 2009.

Creed, I. F., McKnight, D. M., Pellerin, B. A., Green, M. B., Bergamaschi, B. A., Aiken, G. R., Burns, D. A., Findlay, S. E. G., Shanley, J. B., Striegl, R. G., Aulenbach, B. T., Clow, D. W., Laudon, H., McGlynn, B. L., McGuire, K. J., Smith, R. A., Stackpoole, S. M., and Smith, R.: The river as a chemostat: fresh perspectives on dissolved organic matter flowing down the river continuum, Canadian Journal of Fisheries and Aquatic Sciences, 72, 1272-1285, 10.1139/cjfas-2014-0400, 2015.

D'Andrilli, J., Cooper, W. T., Foreman, C. M., and Marshall, A. G.: An ultrahigh-resolution mass spectrometry index to estimate natural organic matter lability, Rapid Commun Mass Spectrom, 29, 2385-2401, 10.1002/rcm.7400, 2015.

D'Arcy, B. J., Rosenqvist, T., Mitchell, G., Kellagher, R., and Billett, S.: Restoration challenges for urban rivers, Water Science and Technology, 55, 1-7, 10.2166/wst.2007.065, 2007.

Declerck, S., De Bie, T., Ercken, D., Hampel, H., Schrijvers, S., Van Wichelen, J., Gillard, V., Mandiki, R., Losson, B., Bauwens, D., Keijers, S., Vyverman, W., Goddeeris, B., De meester, L., Brendonck, L., and Martens, K.: Ecological characteristics of small farmland ponds: Associations with land use practices at multiple spatial scales, Biological Conservation, 131, 523-532, https://doi.org/10.1016/j.biocon.2006.02.024, 2006.

del Campo, R., Gómez, R., and Singer, G.: Dry phase conditions prime wet-phase dissolved organic matter dynamics in intermittent rivers, Limnology and Oceanography, 0, 10.1002/lno.11163, 2019.

Fellman, J. B., Hood, E., and Spencer, R. G. M.: Fluorescence spectroscopy opens new windows into dissolved organic matter dynamics in freshwater ecosystems: A review, Limnology and Oceanography, 55, 2452-2462, https://doi.org/10.4319/lo.2010.55.6.2452, 2010.

Fonvielle, J. A., Giling, D. P., Dittmar, T., Berger, S. A., Nejstgaard, J. C., Lyche Solheim, A., Gessner, M. O., Grossart, H.-P., and Singer, G.: Exploring the Suitability of Ecosystem Metabolomes to Assess Imprints of Brownification and Nutrient Enrichment on Lakes, Journal of Geophysical Research: Biogeosciences, 126, e2020JG005903, https://doi.org/10.1029/2020JG005903, 2021.

Friedland, G., Grüneberg, B., and Hupfer, M.: Geochemical signatures of lignite mining products in sediments downstream a fluvial-lacustrine system, Science of The Total Environment, 760, 143942, https://doi.org/10.1016/j.scitotenv.2020.143942, 2021.

Gessner, M. O., Chauvet, E., and Dobson, M.: A Perspective on Leaf Litter Breakdown in Streams, Oikos, 85, 377-384, 10.2307/3546505, 1999.

Gessner, M. O., Hinkelmann, R., Nützmann, G., Jekel, M., Singer, G., Lewandowski, J., Nehls, T., and Barjenbruch, M.: Urban water interfaces, Journal of Hydrology, 514, 226-232, http://dx.doi.org/10.1016/j.jhydrol.2014.04.021, 2014.

Graeber, D., Gelbrecht, J., Pusch, M. T., Anlanger, C., and von Schiller, D.: Agriculture has changed the amount and composition of dissolved organic matter in Central European headwater streams, Science of The Total Environment, 438, 435-446, https://doi.org/10.1016/j.scitotenv.2012.08.087, 2012.

Hansen, A. M., Kraus, T. E. C., Pellerin, B. A., Fleck, J. A., Downing, B. D., and Bergamaschi, B. A.: Optical properties of dissolved organic matter (DOM): Effects of biological and photolytic degradation, Limnology and Oceanography, 61, 1015-1032, 10.1002/lno.10270, 2016.

~~Helms, J. R., Stubbins, A., Ritchie, J. D., Minor, E. C., Kieber, D. J., and Mopper, K.: Absorption spectral slopes and slope ratios as indicators of molecular weight, source, and photobleaching of chromophoric dissolved organic matter, Limnology and Oceanography, 53, 955-969, 10.4319/lo.2008.53.3.0955, 2008.~~

Huber, S. A., Balz, A., Abert, M., and Pronk, W.: Characterisation of aquatic humic and non-humic matter with size-exclusion chromatography – organic carbon detection – organic nitrogen detection (LC-OCD-OND), Water Research, 45, 879-885, http://dx.doi.org/10.1016/j.watres.2010.09.023, 2011.

Huser, B. J., Futter, M., Lee, J. T., and Perniel, M.: In-lake measures for phosphorus control: The most feasible and cost-effective solution for long-term management of water quality in urban lakes, Water Research, 97, 142-152, https://doi.org/10.1016/j.watres.2015.07.036, 2016.

Hutchins, R. H. S., Aukes, P., Schiff, S. L., Dittmar, T., Prairie, Y. T., and del Giorgio, P. A.: The Optical, Chemical, and Molecular Dissolved Organic Matter Succession Along a Boreal Soil-Stream-River Continuum, Journal of Geophysical Research: Biogeosciences, 122, 2892-2908, 10.1002/2017jg004094, 2017.

Jaffé, R., McKnight, D., Maie, N., Cory, R., McDowell, W. H., and Campbell, J. L.: Spatial and temporal variations in DOM composition in ecosystems: The importance of long-term monitoring of optical properties, Journal of Geophysical Research: Biogeosciences, 113, doi:10.1029/2008JG000683, 2008.

Jespersen, A. M. and Christoffersen, K.: Measurments of chlorophyll-a from phytoplankton using ethanol as extraction solvent. , Archiv für Hydrobiologie, 109, 445-454. , 1987.

Johnson, M.R., and Zelt, R.B., Protocols for Mapping and Characterizing Land Use/Land Cover in RiparianZones: U.S. Geological Survey Open-File Report 2005-1302, 22 p. 2005

Jouanneau, S., Recoules, L., Durand, M. J., Boukabache, A., Picot, V., Primault, Y., Lakel, A., Sengelin, M., Barillon, B., and Thouand, G.: Methods for assessing biochemical oxygen demand (BOD): A review, Water Research, 49, 62-82, https://doi.org/10.1016/j.watres.2013.10.066, 2014.

Kellerman, A. M., Dittmar, T., Kothawala, D. N., and Tranvik, L. J.: Chemodiversity of dissolved organic matter in lakes driven by climate and hydrology, Nature Communications, 5, 3804, 10.1038/ncomms4804, 2014.

Koch, B. P. and Dittmar, T.: From mass to structure: an aromaticity index for high-resolution mass data of natural organic matter, Rapid Communications in Mass Spectrometry, 20, 926-932, https://doi.org/10.1002/rcm.2386, 2006.

Koch, B. P., Dittmar, T., Witt, M., and Kattner, G.: Fundamentals of Molecular Formula Assignment to Ultrahigh Resolution Mass Data of Natural Organic Matter, Analytical Chemistry, 79, 1758-1763, 10.1021/ac061949s, 2007.

Ladwig, R., Heinrich, L., Singer, G., and Hupfer, M.: Sediment core data reconstruct the management history and usage of a heavily modified urban lake in Berlin, Germany, Environmental Science and Pollution Research, 24, 25166-25178, 10.1007/s11356-017-0191-z, 2017.

Lambert, T., Darchambeau, F., Bouillon, S., Alhou, B., Mbega, J.-D., Teodoru, C. R., Nyoni, F. C., Massicotte, P., and Borges, A. V.: Landscape Control on the Spatial and Temporal Variability of Chromophoric Dissolved Organic Matter and Dissolved Organic Carbon in Large African Rivers, Ecosystems, 18, 1224-1239, 10.1007/s10021-015-9894-5, 2015.

Larson, J. H., Frost, P. C., Xenopoulos, M. A., Williams, C. J., Morales-Williams, A. M., Vallazza, J. M., Nelson, J. C., and Richardson, W. B.: Relationships between land cover and dissolved organic matter change along the river to lake transition, Ecosystems, 17, 1413-1425, 10.1007/s10021-014-9804-2, 2014.

Legendre, P. and Legendre, L.: Numerical ecology, 3rd English edition. Elsevier Science, 2012.

Lesaulnier, C. C., Herbold, C. W., Pelikan, C., Berry, D., Gérard, C., Le Coz, X., Gagnot, S., Niggemann, J., Dittmar, T., Singer, G. A., and Loy, A.: Bottled aqua incognita: microbiota assembly and dissolved organic matter diversity in natural mineral waters, Microbiome, 5, 126, 10.1186/s40168-017-0344-9, 2017.

Loiselle, S. A., Bracchini, L., Dattilo, A. M., Ricci, M., Tognazzi, A., Cózar, A., and Rossi, C.: The optical characterization of chromophoric dissolved organic matter using wavelength distribution of absorption spectral slopes, Limnology and Oceanography, 54, 590-597, 10.4319/lo.2009.54.2.0590, 2009.

Maranger, R. and Pullin, M. J.: 8 - Elemental Complexation by Dissolved Organic Matter in Lakes: Implications for Fe Speciation and the Speciation and the Bioavailability of Fe and P, in: Aquatic Ecosystems, edited by: Findlay, S. E. G., and Sinsabaugh, R. L., Academic Press, Burlington, 185-214, https://doi.org/10.1016/B978-012256371-3/50009-3, 2003.

Mardia, K. V., Kent, J.T. and Bibby, J.M. : Multivariate Analysis, 1979.

~~McKnight, D. M., Boyer, E. W., Westerhoff, P. K., Doran, P. T., Kulbe, T., and Andersen, D. T.: Spectrofluorometric characterization of dissolved organic matter for indication of precursor organic material and aromaticity, Limnology and Oceanography, 46, 38-48, 10.4319/lo.2001.46.1.0038, 2001.~~

Murphy, K. R., Stedmon, C. A., Wenig, P., and Bro, R.: OpenFluor– an online spectral library of auto-fluorescence by organic compounds in the environment, Analytical Methods, 6, 658-661, 10.1039/C3AY41935E, 2014.

Murphy, K. R., Hambly, A., Singh, S., Henderson, R. K., Baker, A., Stuetz, R., and Khan, S. J.: Organic Matter Fluorescence in Municipal Water Recycling Schemes: Toward a Unified PARAFAC Model, Environmental Science & Technology, 45, 2909-2916, 10.1021/es103015e, 2011.

Nega, M., Braun, B., Künzel, S., and Szewzyk, U.: Evaluating the Impact of Wastewater Effluent on Microbial Communities in the Panke, an Urban River, Water, 11, 888, https://doi.org/10.3390/w11050888, 2019.

Ohno, T.: Fluorescence Inner-Filtering Correction for Determining the Humification Index of Dissolved Organic Matter, Environmental Science & Technology, 36, 742-746, 10.1021/es0155276, 2002.

~~Osburn, C. L., Wigdahl, C. R., Fritz, S. C., and Saros, J. E.: Dissolved organic matter composition and photoreactivity in prairie lakes of the U.S. Great Plains, Limnology and Oceanography, 56, 2371-2390, 10.4319/lo.2011.56.6.2371, 2011.~~

Park, J.-H.: Spectroscopic characterization of dissolved organic matter and its interactions with metals in surface waters using size exclusion chromatography, Chemosphere, 77, 485-494, https://doi.org/10.1016/j.chemosphere.2009.07.054, 2009.

Parlanti, E., Wörz, K., Geoffroy, L., and Lamotte, M.: Dissolved organic matter fluorescence spectroscopy as a tool to estimate biological activity in a coastal zone submitted to anthropogenic inputs, Organic Geochemistry, 31, 1765-1781, http://dx.doi.org/10.1016/S0146-6380(00)00124-8, 2000.

Peres-Neto, P. R. and Jackson, D. A.: How well do multivariate data sets match? The advantages of a Procrustean superimposition approach over the Mantel test, Oecologia, 129, 169-178, 10.1007/s004420100720, 2001.

Peter, H., Singer, G., Ulseth, A. J., Dittmar, T., Prairie, Y. T., and Battin, T. J.: Travel Time and Source Variation Explain the Molecular Transformation of Dissolved Organic Matter in an Alpine Stream Network, Journal of Geophysical Research: Biogeosciences, 125, e2019JG005616, https://doi.org/10.1029/2019JG005616, 2020.

Peterson, E., Merton, A., Theobald, D., and Urquhart, N. S.: Patterns of Spatial Autocorrelation in Stream Water Chemistry, Environ Monit Assess, 121, 571-596, 10.1007/s10661-005-9156-7, 2006.

Peuravuori, J. and Pihlaja, K.: Molecular size distribution and spectroscopic properties of aquatic humic substances, Analytica Chimica Acta, 337, 133-149, https://doi.org/10.1016/S0003-2670(96)00412-6, 1997.

QGIS Development Team: QGIS Geographic Information System. Open Source Geospatial Foundation Project. http://qgis.osgeo.org, 2017.

R Core Team: R: A language and environment for statistical computing. R Foundation for Statistical Computing, Vienna, Austria. URL https://www.R-project.org/, 2016.

Riedel, T. and Dittmar, T.: A Method Detection Limit for the Analysis of Natural Organic Matter via Fourier Transform Ion Cyclotron Resonance Mass Spectrometry, Analytical Chemistry, 86, 8376-8382, 10.1021/ac501946m, 2014.

Sankar, M. S., Dash, P., Lu, Y., Mercer, A. E., Turnage, G., Shoemaker, C. M., Chen, S., and Moorhead, R. J.: Land use and land cover control on the spatial variation of dissolved organic matter across 41 lakes in Mississippi, USA, Hydrobiologia, 847, 1159-1176, 10.1007/s10750-019-04174-0, 2020.

Savory, J. J., Kaiser, N. K., McKenna, A. M., Xian, F., Blakney, G. T., Rodgers, R. P., Hendrickson, C. L., and Marshall, A. G.: Parts-Per-Billion Fourier Transform Ion Cyclotron Resonance Mass Measurement Accuracy with a "Walking" Calibration Equation, Analytical Chemistry, 83, 1732-1736, 10.1021/ac102943z, 2011.

Schwarzenbach, R. P., Escher, B. I., Fenner, K., Hofstetter, T. B., Johnson, C. A., Gunten, U. v., and Wehrli, B.: The Challenge of Micropollutants in Aquatic Systems, Science, 313, 1072-1077, 10.1126/science.1127291, 2006.

Spencer, R. G. M., Stubbins, A., Hernes, P. J., Baker, A., Mopper, K., Aufdenkampe, A. K., Dyda, R. Y., Mwamba, V. L., Mangangu, A. M., Wabakanghanzi, J. N., and Six, J.: Photochemical degradation of dissolved organic matter and dissolved lignin phenols from the Congo River, Journal of Geophysical Research: Biogeosciences, 114, 10.1029/2009jg000968, 2009.

Stanley, E. H., Powers, S. M., Lottig, N. R., Buffam, I., and Crawford, J. T.: Contemporary changes in dissolved organic carbon (DOC) in human-dominated rivers: is there a role for DOC management?, Freshwater Biology, 57, 26-42, 10.1111/j.1365-2427.2011.02613.x, 2012.

Stedmon, C. A. and Bro, R.: Characterizing dissolved organic matter fluorescence with parallel factor analysis: a tutorial, Limnology and Oceanography: Methods, 6, 572-579, 10.4319/lom.2008.6.572, 2008.

Stedmon, C. A. and Markager, S.: Tracing the production and degradation of autochthonous fractions of dissolved organic matter by fluorescence analysis, Limnology and Oceanography, 50, 1415-1426, 10.4319/lo.2005.50.5.1415, 2005.

Tamil Selvi, S., Raman, V., and Rajendran, N.: Corrosion inhibition of mild steel by benzotriazole derivatives in acidic medium, Journal of Applied Electrochemistry, 33, 1175-1182, 10.1023/B:JACH.0000003852.38068.3f, 2003.

Teymouri, B.: Fluorescence spectroscopy and parallel factor analysis of waters from municipal waste sources, Thesis presented to the Faculty of the Graduate School at the University of Missouri – Columbia, 2007.

Thurman, E. M.: Classification of Dissolved Organic Carbon, in: Organic Geochemistry of Natural Waters, edited by: Thurman, E. M., Springer Netherlands, Dordrecht, 103-110, 10.1007/978-94-009-5095-5_5, 1985.

Tufekcioglu, M., Schultz, R. C., Isenhart, T. M., Kovar, J. L., and Russell, J. R.: Riparian Land-Use, Stream Morphology and Streambank Erosion within Grazed Pastures in Southern Iowa, USA: A Catchment-Wide Perspective, Sustainability, 12, 6461, 2020.

Weishaar, J. L., Aiken, G. R., Bergamaschi, B. A., Fram, M. S., Fujii, R., and Mopper, K.: Evaluation of Specific Ultraviolet Absorbance as an Indicator of the Chemical Composition and Reactivity of Dissolved Organic Carbon, Environmental Science & Technology, 37, 4702-4708, 10.1021/es030360x, 2003.

Weyhenmeyer, G. A., Prairie, Y. T., and Tranvik, L. J.: Browning of Boreal Freshwaters Coupled to Carbon-Iron Interactions along the Aquatic Continuum, PLOS ONE, 9, e88104, 10.1371/journal.pone.0088104, 2014.

White, J. Y. and Walsh, C. J.: Catchment-scale urbanization diminishes effects of habitat complexity on instream macroinvertebrate assemblages, Ecological Applications, 30, e2199, 10.1002/eap.2199, 2020.

Williams, C. J., Frost, P. C., and Xenopoulos, M. A.: Beyond best management practices: pelagic biogeochemical dynamics in urban stormwater ponds, Ecological Applications, 23, 1384-1395, 10.1890/12-0825.1, 2013.

Williams, C. J., Frost, P. C., Morales-Williams, A. M., Larson, J. H., Richardson, W. B., Chiandet, A. S., and Xenopoulos, M. A.: Human activities cause distinct dissolved organic matter composition across freshwater ecosystems, Global Change Biology, 22, 613-626, 10.1111/gcb.13094, 2016.

Wilson, H. F. and Xenopoulos, M. A.: Effects of agricultural land use on the composition of fluvial dissolved organic matter, Nature Geoscience, 2, 37-41, 10.1038/ngeo391, 2009.

Xenopoulos, M. A., Barnes, R. T., Boodoo, K. S., Butman, D., Catalán, N., D'Amario, S. C., Fasching, C., Kothawala, D. N., Pisani, O., Solomon, C. T., Spencer, R. G. M., Williams, C. J., and Wilson, H. F.: How humans alter dissolved organic matter composition in freshwater: relevance for the Earth's biogeochemistry, Biogeochemistry, 154, 323-348, 10.1007/s10533-021-00753-3, 2021.

Yamashita, Y., Scinto, L. J., Maie, N., and Jaffé, R.: Dissolved Organic Matter Characteristics Across a Subtropical Wetland's Landscape: Application of Optical Properties in the Assessment of Environmental Dynamics, Ecosystems, 13, 1006-1019, 10.1007/s10021-010-9370-1, 2010.

Zietzschmann, F., Aschermann, G., and Jekel, M.: Comparing and modeling organic micro-pollutant adsorption onto powdered activated carbon in different drinking waters and WWTP effluents, Water Research, 102, 190-201, http://dx.doi.org/10.1016/j.watres.2016.06.041, 2016.